



TECHNISCHE
UNIVERSITÄT
WIEN

Master Thesis

ASYMMETRIC AZIRIDINATION OF CYCLIC ENONES VIA COUNTERION ENHANCED ORGANOCATALYSIS

Ausgeführt am

Institut für Angewandte Synthesechemie

unter der Leitung von

Assoc. Prof. Dipl.-Ing. Dr.techn. Katharina Schröder

eingereicht an der Technischen Universität Wien

am 26.02.2021

von

Melanie Weisz BSc.

Matrikelnummer: 01446482

Kastanienweg 10

2852 Hochneukirchen

Table of Contents

Table of Contents	i
Abstract	iii
1 Introduction	1
1.1 Aziridines	1
1.1.1 Properties of aziridines	1
1.1.2 Usage of aziridines	3
1.1.3 Preparation of aziridines	4
1.2 Organocatalysis	7
1.2.1 Enamine catalysis	10
1.2.2 Iminium catalysis	12
1.2.3 Iminium-enamine tandem catalysis	14
1.2.4 Singly occupied molecular orbital catalysis	16
1.2.5 Asymmetric counteranion directed catalysis	17
1.3 Counterion enhanced organocatalysis	21
2 State of the art	23
3 Aim of the thesis	24
4 Results and discussion	25
4.1 Catalyst optimization	25
4.1.1 Screening of the amine-functionality	25
4.1.2 Screening of the phosphoric acid anion	27
4.1.3 Catalyst screening	29
4.2 Optimization of the reaction conditions	33
4.2.1 Optimization of the base and base equivalents	33
4.2.2 Optimization of the solvent	34
4.3 Reactant optimization	36
4.4 Catalyst synthesis	38
4.4.1 Diamine synthesis	38
4.4.2 Phosphoric acid synthesis	39
4.5 Substrate scope and limitations	41
4.6 Mechanism	43

5	Conclusion	45
6	Experimental Part	46
6.1	Materials and Methods	46
6.2	Reactant synthesis	47
6.2.1	<i>tert</i> -Butyl hydroxycarbamate (2)	47
6.2.2	<i>tert</i> -Butyl (tosyloxy)carbamate (3)	48
6.2.3	<i>tert</i> -Butyl acetoxycarbamate (4)	49
6.3	Diamine synthesis	50
6.3.1	1-Cyano-2-ethoxy-2-oxoethanaminium 4-methylbenzenesulfonate (14) .	50
6.3.2	(<i>R</i>)-2-((<i>tert</i> -Butoxycarbonyl)amino)-2-phenylacetic acid (16)	51
6.3.3	(<i>S</i>)-2-((<i>tert</i> -Butoxycarbonyl)amino)-2-phenylacetic acid (18)	52
6.3.4	<i>tert</i> -Butyl-(<i>R</i>)-(2-oxo-1-phenyl-2-(piperidin-1-yl)ethyl)carbamate (19) .	53
6.3.5	<i>tert</i> -Butyl-(<i>S</i>)-(2-oxo-1-phenyl-2-(piperidin-1-yl)ethyl)carbamate (20) .	54
6.3.6	(<i>R</i>)-1-Phenyl-2-(piperidin-1-yl)ethan-1-amine (22)	55
6.3.7	(<i>S</i>)-1-Phenyl-2-(piperidin-1-yl)ethan-1-amine (24)	56
6.4	Phosphoric acid synthesis	57
6.4.1	6,6'-((2-Methoxyphenyl)methylene)bis(2-(<i>tert</i> -butyl)-4-methylphenol) (32)	57
6.4.2	4,8-Di- <i>tert</i> -butyl-6-hydroxy-12-(2-methoxyphenyl)-2,10-dimethyl-12 <i>H</i> - dibenzo[<i>d,g</i>][1,3,2]dioxaphosphocine 6-oxide (33)	58
6.5	Asymmetric aziridination of cyclic enones	59
6.5.1	General procedure for parameter optimization	59
6.5.2	General procedure for scope and limitations	60
6.5.3	Analytical data of the aziridines	61
7	Appendix	66
7.1	HPLC-spectra	66
7.1.1	<i>tert</i> -Butyl-2-oxo-7-azabicyclo[4.1.0]heptane-7-carboxylate	66
7.1.2	<i>tert</i> -Butyl-1-methyl-5-oxo-7-azabicyclo[4.1.0]heptane-7-carboxylate . .	68
7.1.3	<i>tert</i> -Butyl-1-benzyl-5-oxo-7-azabicyclo[4.1.0]heptane-7-carboxylate . . .	70
7.1.4	<i>tert</i> -Butyl-2,2-dimethyl-5-oxo-7-azabicyclo[4.1.0]heptane-7-carboxylate	72
7.2	List of abbreviations	74
7.3	List of figures	76
7.4	List of tables	79
8	References	80

Abstract

The focus of the present thesis is the asymmetric aziridination of cyclic enones via counterion enhanced organocatalysis. In this approach, the catalyst system consists of a chiral diamine, which can be obtained from an amino-acid precursor, and an achiral phosphoric acid, which combine to form the catalyst salt. In order to determine the best performing catalyst system and the optimal reaction conditions, several amines, phosphoric acids, bases and solvents were screened. After optimizing the parameters, the asymmetric aziridination was successfully applied to a range of 3- and 4-substituted cyclohexenone substrates, in a final step. With this new catalyst system, excellent enantioselectivities as well as good yields could be achieved for several substrates and consequently, the versatility of the concept of counterion enhanced organocatalysis could be demonstrated.

Kurzfassung

Der Fokus der vorliegenden Arbeit ist die asymmetrische Aziridinerung mittels Gegenion-dirigierender Organokatalyse. Bei dieser Methode setzt sich das Katalysatorsystem aus einem chiralen Diamin, welches aus einer Aminosäure als Vorläufersubstanz erhalten werden kann, und einer nicht chiralen Phosphorsäure zusammen, welche gemeinsam das Katalysatorsalz bilden. Um das beste Katalysatorsystem, sowie die optimalen Reaktionsbedingungen zu bestimmen, wurden verschiedene Amine, Phosphorsäuren, Basen und Lösungsmittel untersucht. Nach der Optimierung dieser Parameter, konnte die asymmetrische Aziridinerung in einem letzten Schritt erfolgreich auf einige 3- und 4-substituierte Cyclohexenone angewendet werden. Mit dem neuen Katalysatorsystem konnten exzellente Enantioselektivitäten, sowie gute Ausbeuten erreicht werden und somit konnte die Vielseitigkeit der Gegenion-dirigierenden Organokatalyse demonstriert werden.

1 Introduction

1.1 Aziridines

Aziridines, the nitrogen analogues of epoxides, are the smallest nitrogen-containing heterocycles and are useful building blocks in synthetic chemistry. Apart from their role as crucial precursors of complex molecules, they are also found in the scaffold of natural products, which makes them also interesting synthetic targets for total synthesis.^{1,2}

1.1.1 Properties of aziridines

Since aziridines are saturated three-membered hetero-cycles, which contain an amine group, they exhibit ring strain similarly to other three-membered rings, e. g., epoxides or cyclopropanes (Figure 1).^{1,3}

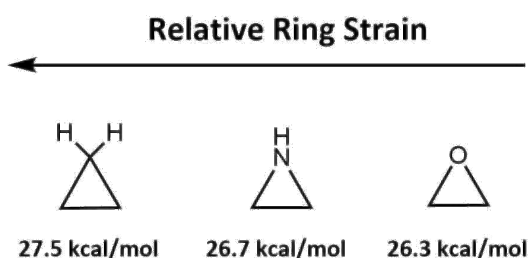
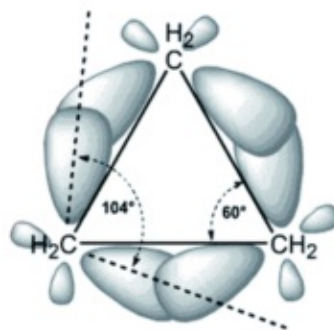
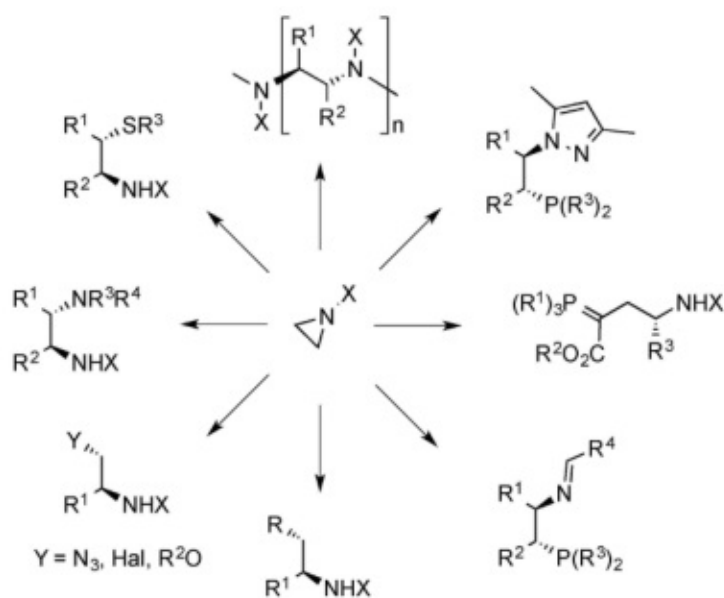


Figure 1: Ring strains in three-membered rings.³

Due to the enormous angle strains, the bonds are bent outwards to form the so called “banana” bonds. As a result, the s-character in the bonds gets increased³ and compared to a normal sp^3 carbon bond, the bond angles in aziridines, which are about 60° , are substantially smaller (Figure 2).¹

Figure 2: "Banana" shaped bonds.³

The resulting ring strains coupled with the electronegativity of the nitrogen atom render aziridines susceptible to ring-opening reactions with nucleophiles, even under mild conditions. As a result, many regio- and stereoselective functionalities can be obtained (Figure 3).¹

Figure 3: Ring opening reactions of aziridines.¹

Such aziridine ring-opening reactions are used in industrial production of a wide range of bulk chemicals, for instance, polyethylenimine, epoxy resins or ethylene glycol.¹ Furthermore the ring strain of these heterocycles makes them important precursors of more complex molecules and many important nitrogen-containing compounds, like amines, amino alcohols or amino acids, can be obtained.²

1.1.2 Usage of aziridines

Apart from their use in the industrial production of bulk chemicals, the aziridine scaffold is also part of several drug candidates and biologically active molecules.^{1,4} Particularly, the antitumor and antibiotic properties of a wide range of naturally-occurring aziridine-bearing compounds make them interesting synthetic targets and furthermore, structure-activity relationships have shown that the aziridine ring plays an essential role in this antitumor activity.^{2,4,5} Important examples for such biologically active aziridines are albomitomycin and isomitomycin, which work as neoplasm inhibitors. Due to the easy chemical transformation of aziridines, their ring-expansion became a key step in the total synthesis of a wide range of natural biologically-active compounds, such as mannostatin and allosamidin, which are used similarly to glycosidase inhibitors (Figure 4).¹

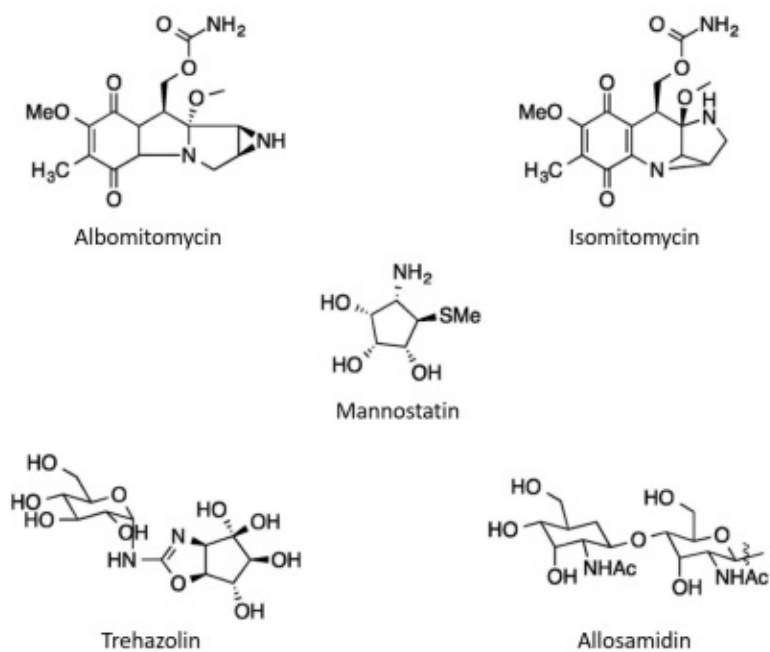


Figure 4: Examples of biologically-active aziridine-containing compounds and compounds obtained from aziridines.¹

1.1.3 Preparation of aziridines

As a result of the growing importance of aziridines as crucial intermediates in asymmetric synthesis, various synthetic pathways have been developed for the synthesis of aziridines over the past years,¹ starting off with the first reported asymmetric catalytic aziridination of olefins, which was carried out by Evans in 1994, with $[N-(p\text{-toluenesulfonyl})\text{imino}]$ phenyliodinane as the nitrene source and a $[\text{bis}(\text{oxazoline})]\text{Cu}$ complex as the catalyst (Figure 5).^{1,6} Such direct aziridination of olefins, in analogy to the epoxidation of alkenes, relies on the metal-mediated transfer of nitrene derivatives to olefins. Nitrenes, where the nitrogen has one electron-withdrawing substituent and two electron-lone pairs, are used. Such nitrenes can be obtained from a wide range of nitrene sources, for example, aryl azides, sulfonyl azides, imino iodinanes, halo amines and tosyloxy carbamates, and are very reactive intermediates. For the aziridination process, catalytic amounts of the metal are needed, as well as ligands, which are often porphyrins, bisoxazolines, acetylacetone, imines or diimines.²

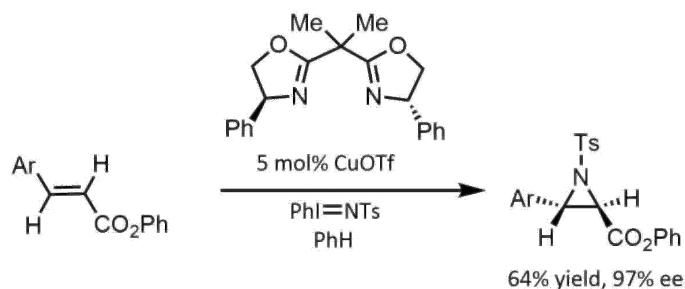


Figure 5: Asymmetric catalytic aziridination performed by Evans.⁶

Aziridines can also be prepared from enantiomerically-pure epoxides as precursors, for example, the phosphine-mediated ring-closure reaction of 1,2-azidoalcohols, in which the azidoalcohols can be produced from chiral epoxides via several azide sources. Hydroxyazide reacts with trialkyl- or triarylphosphine giving oxazaphospholidines which are then converted to the N-unsubstituted aziridine product after heating in acetonitrile (Figure 6). During the reaction, both stereocenters of the product are inverted and this method works for several different substrates.⁵

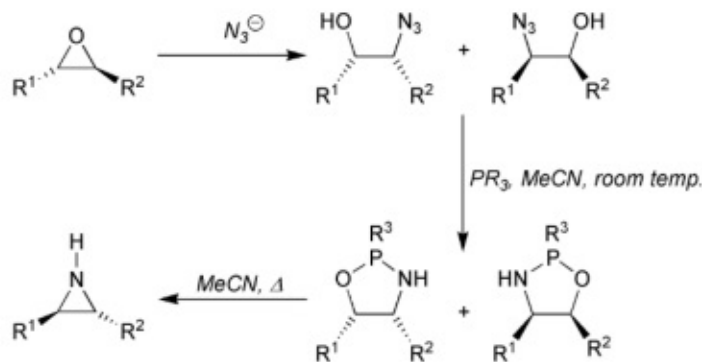


Figure 6: Asymmetric aziridines produced from 1,2-azidoalcohols.⁵

Other methodologies for the synthesis of aziridines are the addition of carbenes or ylides to imines. The reaction of carbenes, especially those obtained from diazo compounds with imines, is already quite known and its high stereoselectivity, easy implementation and good yields make this method very attractive. Apart from transition metal complexes, it has been reported that these reactions can also be catalyzed by Lewis acids, Brønsted acids as well as ionic liquids and lithium perchlorate.⁴ In terms of transition metal catalysis, it has been shown that copper and rhodium catalysts are needed and especially the groups of Jacobsen⁷ and Jørgensen⁸ achieved good results using copper salts in combination with chiral bis-oxazoline ligands. More recently, the group of Zhang⁹ used diazoacetate derivatives and *N-p*-methoxyphenyl imines to obtain highly functionalized aziridines. High yields and good diastereoselectivity could be achieved by using dirhodium tetraacetate as a catalyst (Figure 7).²

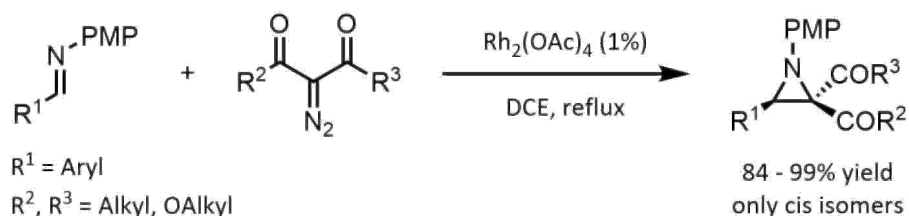


Figure 7: Aziridine synthesis via carbene addition to imines.²

Additionally, the use of ylides instead of carbenes is an effective method for the preparation of asymmetric aziridines. For these aziridination reactions, mainly sulfur ylides are used and the reaction can either be performed with chiral sulfur ylides or with chiral imines as auxiliary. An example for the use of chiral imines as the auxiliary is the asymmetric aziridination of chiral *N-tert*-butanesulfinylimines which has been reported by the group of Mayer.¹⁰ The reaction uses benzyl-stabilized sulfur ylides, which are created in situ from the decomposition of phenyldiazomethane, and it is catalyzed by the rhodium catalyst in the presence of sulfides, e. g.,

tetrahydrothiophene and dibutyl sulfide (Figure 8). The desired aziridines could be obtained with excellent yields and a wide range of substrates.⁴

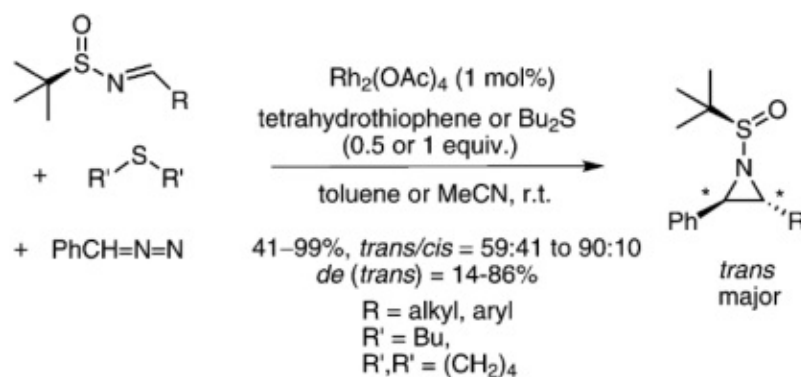


Figure 8: Aziridine synthesis via ylide addition to imines.⁴

Apart from the metal-mediated methods for the asymmetric catalytic aziridination, recently, organocatalytic ways to synthesize chiral aziridines became popular, particularly, the asymmetric aziridination of α,β -unsaturated carbonyl compounds via covalent catalysis using an aminocatalyst. The general reaction scheme for such organocatalytic reactions is shown in Figure 9.¹

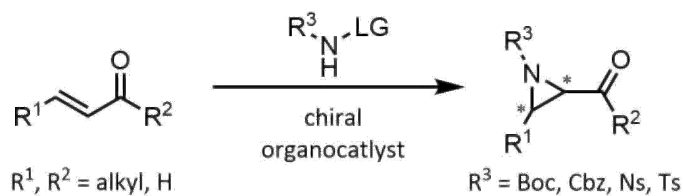


Figure 9: General scheme for the organocatalytic asymmetric aziridination of α,β -unsaturated carbonyl compounds.¹

1.2 Organocatalysis

Since the beginning of the 21st century, the enantioselective synthesis of molecules became a central topic in research. Due to the rising importance of chiral compounds as optical and electronic devices, as enantiomerically pure pharmaceuticals or as components in polymers, asymmetric catalysis started to play a prominent role. Asymmetric catalysis uses chiral catalysts which accelerate the reaction in a way that one enantiomer is formed preferentially. For a long period of time, transformations based on transition-metal complexes and enzymes were considered to be the main two classes of highly effective asymmetric catalysis. Nevertheless, within the last twenty years, the field of organocatalysis emerged as a third class of efficient asymmetric transformations (Figure 10).^{11,12}

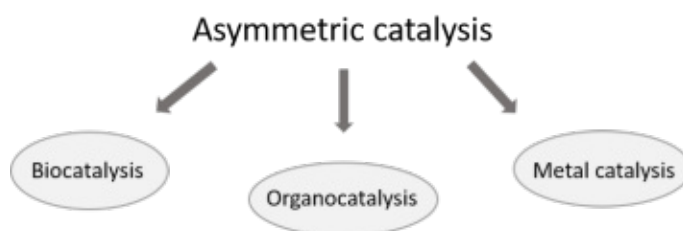


Figure 10: The three classes of asymmetric catalysis.

Organocatalysis is the use of small organic molecules to catalyze organic transformations. Although organocatalytic transformations were already sporadically reported in the 1900s, the research interest in this topic just started to arouse in the 2000s and it was also in 2000 when MacMillan first used the term organocatalysis.¹³ The first asymmetric organocatalytic transformation was already reported in 1912, when Bredig and Fiske were able to carry out an enantioselective cyanohydrin synthesis.¹² The addition of HCN to benzaldehyde was catalyzed by quinine and quinidine (Figure 11) and gave the cyanohydrins with opposite enantioselectivity.¹⁴

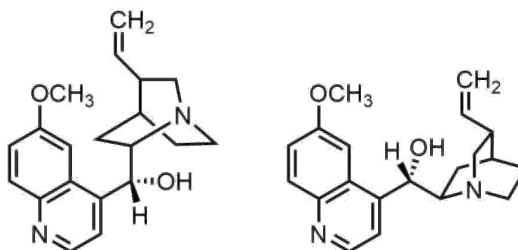


Figure 11: Quinine and quinidine, used as organocatalysts.¹⁴

In 1960, Pracejus could report an organocatalytic reaction that achieved significant enantioselectivities. The addition of methanol to phenylmethylketene with again an alkaloid catalyst,

namely *O*-acetylquinine, could be carried out successfully with 74% ee and only 1 mol% of the catalyst (Figure 12).¹⁴

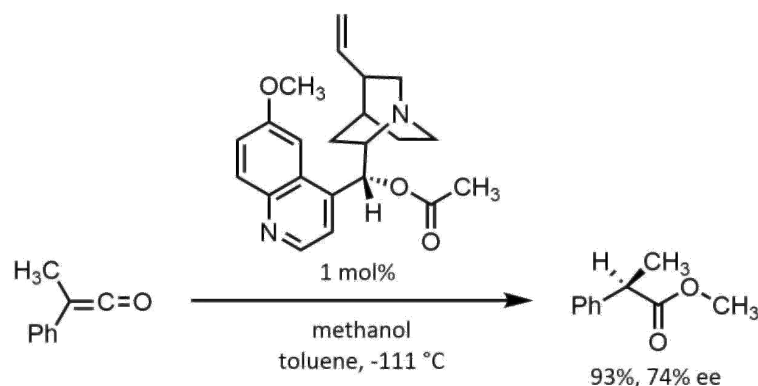


Figure 12: Organocatalytic addition of methanol to phenylmethylketene.¹⁴

In 1971, a milestone in the field of asymmetric organocatalysis could be achieved by the first catalytic aldol reaction, the Hajos-Parrish-Eder-Sauer-Wiechert reaction (Figure 13). This enantioselective reaction uses the simple amino acid L-proline as catalyst, which later on was used in a wide range of remarkable chemo- and enantioselective reactions by List and MacMillan.¹⁴

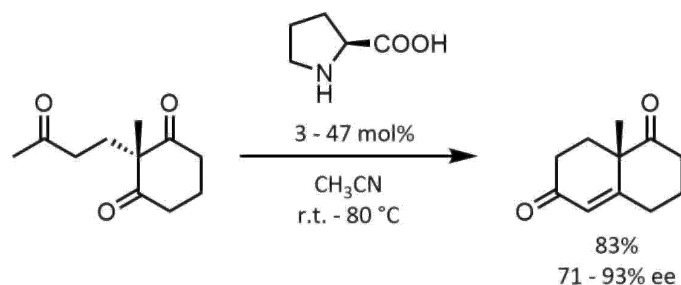


Figure 13: Hajos-Parrish-Eder-Sauer-Wiechert reaction.¹⁴

Based on the work that has been done already in the 1900s, a lot of ground-breaking work and different organocatalytic catalysts have been reported by the groups of List, MacMillan and others in the beginning of 2000, and by now the field of asymmetric organocatalysis has experienced a massive growth and has become a powerful tool in asymmetric catalysis.¹⁴

Although the field of organocatalysis is relatively new and not so well established, there are already a few advantages compared to the commonly used method of transition-metal catalysis (Table 1). Contrary to the transition-metal-based catalysis, organocatalysis uses mild reaction conditions and the catalysts are inert towards moisture and oxygen, which allows their easier handling compared to the often sensitive transition-metal catalysts. Furthermore,

since organocatalysis does not need expensive and toxic metals, metal contamination can be avoided, giving an especially attractive method, for example, for the preparation of pharmaceutical products, where metal contamination is not tolerated. Another significant advantage is the fact that organocatalysts are either readily available or can be easily and cheaply prepared from precursors of the chiral pool. Nonetheless, there are also some disadvantages considering organocatalysis, for example, high catalyst loading that can get as high as 20 mol% or low catalytic activity which can lead to a lower conversion. Another point is the limited substrate and reaction scope since organocatalysis is still a relatively premature field.¹⁵

Table 1: Comparison between organocatalysis and transition-metal catalysis.¹⁵

Organocatalysis	Transition-metal catalysis
robust	broad substrate scope
inexpensive	high catalytic activity
readily available or easy preparation	low catalyst loading
nontoxic	well established
easy handling; inert towards moisture and oxygen	
no metal contamination	

The field of organocatalysis can be roughly divided into two broad subgroups, the covalent activation mode and the non-covalent activation mode (Figure 14). Within the covalent activation mode, the interaction of the catalyst with the substrate takes place via covalent bonding and within this subgroup again two separate fields can be worked out, namely, amino catalysis and the carbene activation. In amino catalysis, an amine catalyst generally binds to a carbonyl group of the substrate giving an enamine intermediate which can then react further. On the other hand, there is the field of the non-covalent activation mode, where the interaction between catalyst and substrate can either occur through well-defined hydrogen-bonding interactions or, as in the field of coulombic interactions, via electrostatic forces.^{13, 16}

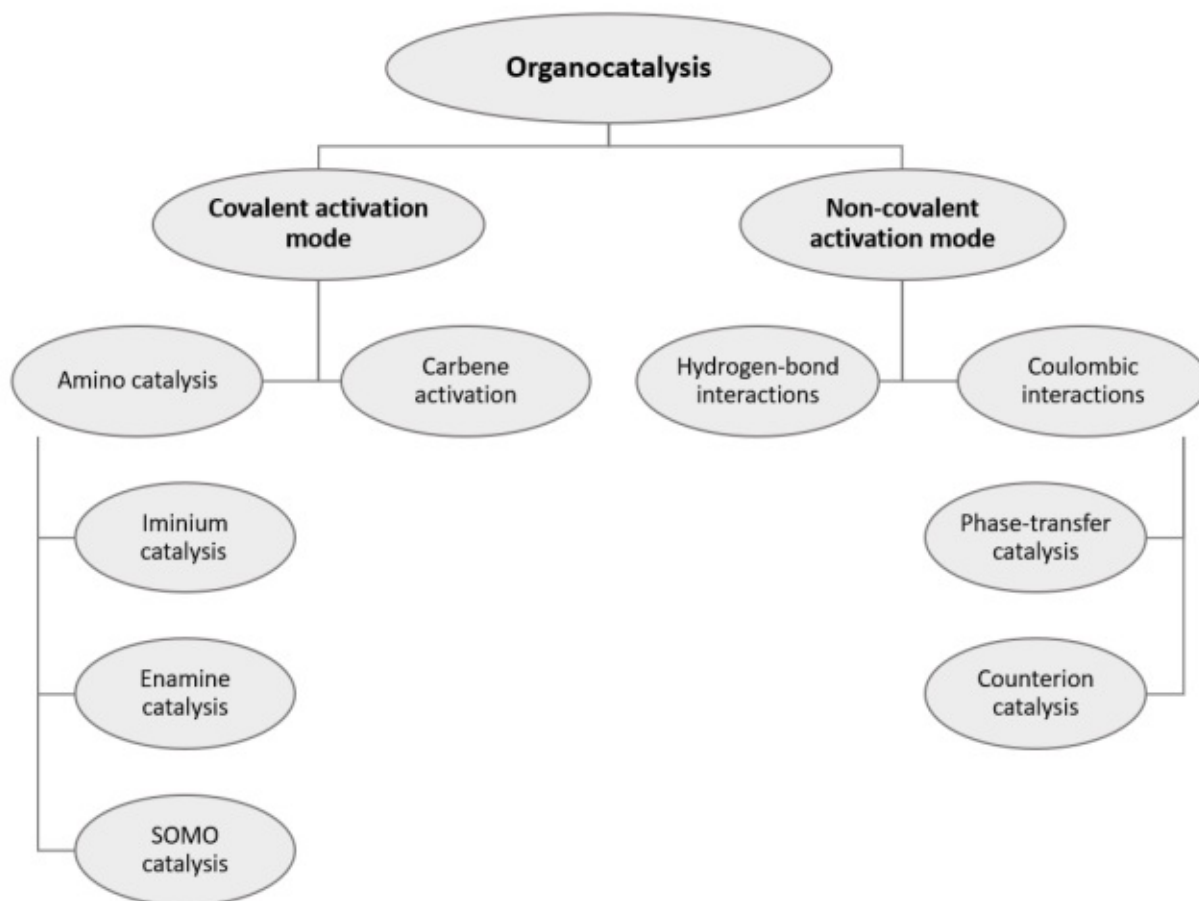


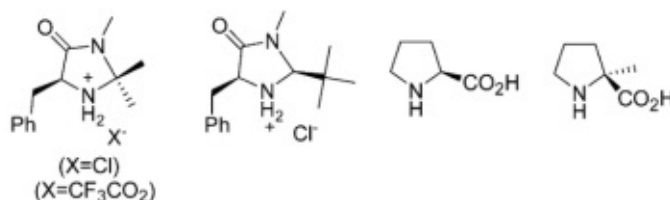
Figure 14: Overview of organocatalytic activation modes.

In the following sections, the field of amino catalysis, containing enamine, iminium and SOMO catalysis, as well as counterion catalysis, will be discussed in more detail.

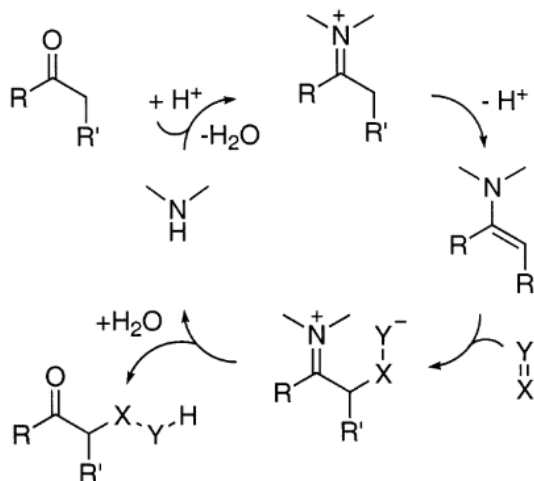
1.2.1 Enamine catalysis

In enamine catalysis, the basis is a reversible generation of enamines from a catalytic amount of amine and a carbonyl compound. A key part in the formation of the enamine is played by the increase of the energy level of the HOMO (highest occupied molecular orbital) and the resulting increase in C-H acidity upon the initial conversion of the carbonyl group into the iminium ion. The first example of an asymmetric enamine catalysis was the Hajos-Parrish-Eder-Sauer-Wiechert reaction, nevertheless, it took another 30 years until the underlying activation mode was exploited for other reactions by the work of Barbas, Lerner and List, who proved the broad applicability of this activation mode through the enamine catalyzed α -functionalization of carbonyl compounds.^{17,13} Some catalysts that are used in enamine catalysis are shown in

Figure 15.

Figure 15: Examples of catalysts used in enamine catalysis.¹⁸

At the beginning of the catalytic cycle, the chiral secondary amine catalyst and the carbonyl compound condense to form an iminium ion (Figure 16). Through the increased acidity of the α -protons, due to the formed iminium ion, the formation of the enamine intermediate via deprotonation is facilitated. The formed intermediate can now attack an electrophile ($X=Y$) and an iminium ion is again formed. After hydrolysis of the new iminium ion with in situ-generated water, the carbonyl product gets liberated and the secondary amine catalyst can reenter the catalytic cycle.¹⁹

Figure 16: Catalytic cycle of the enamine activation.¹⁷

Two different approaches of the electrophilic attack, based on the structure of the catalyst, have been proposed (Figure 17). With proline as the catalyst in reactions in which the electrophile has an electronegative heteroatom, H-bond interactions have been proposed to be responsible for the observed stereoselection. This can be ascribed to the fact that the heteroatom at the electrophile has an electron-pair that can act as an H-bond acceptor, leading to a *Re*-face attack. On the other hand, pyrrolidine catalysts with bulky substituents in position 2 are proposed to direct the incoming electrophile by steric interactions via a *Si*-face attack. This

is also the reason why, even if the H-bond-catalyst and the steric directing catalyst have the same stereochemistry, the reaction will always give different enantiomers of the product.¹⁹

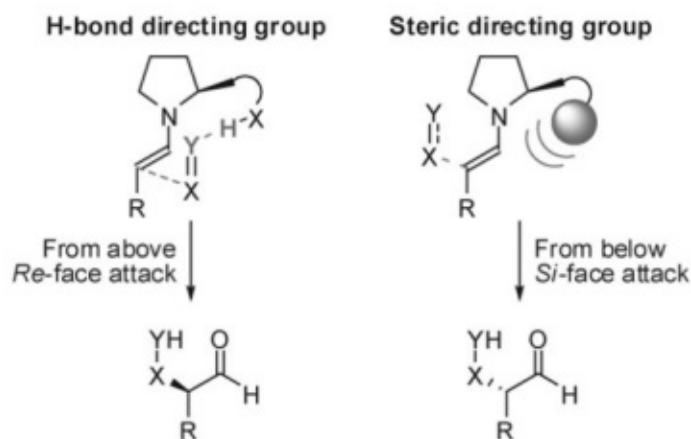
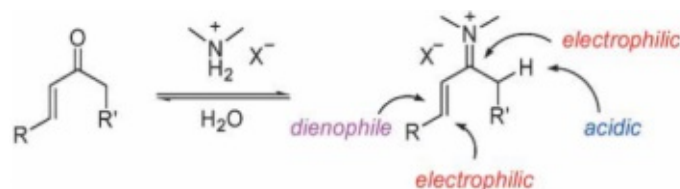


Figure 17: H-bond vs steric directing group.¹⁹

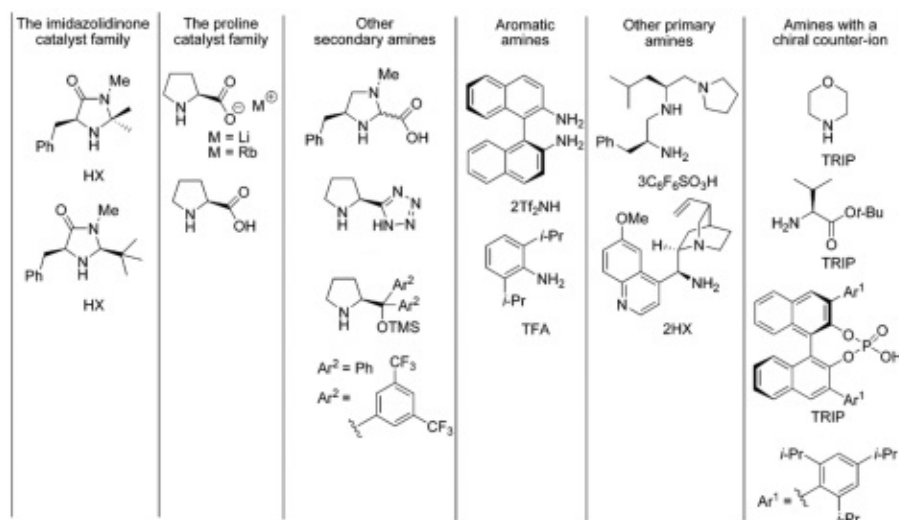
The proline catalyzed enantioselective intermolecular aldol reactions, Mannich reactions and Michael additions, discovered by the groups of List and others, extended the concept of enamine catalysis to other highly enantioselective reactions, such as α -functionalizations of aldehydes and ketones, namely, aminations, hydroxylations, alkylations, chlorinations and intramolecular Micheal reactions.¹⁸

1.2.2 Iminium catalysis

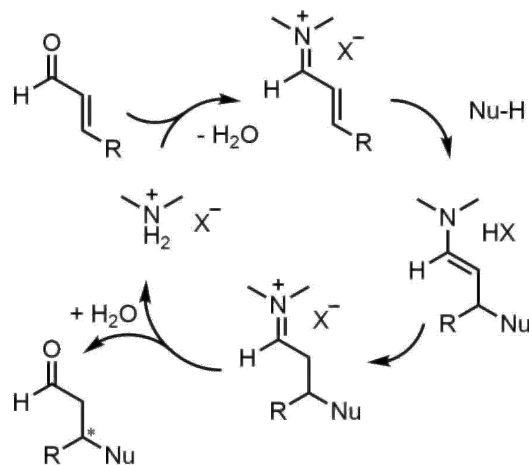
In iminium catalysis, the active species is an iminium ion which is formed via a reversible reaction of an α - β -unsaturated carbonyl compound and an amine catalyst.¹⁶ Generally, even though primary amines, as well as secondary amines, can be used as catalysts secondary amines are more commonly used.²⁰ Through the formation of the iminium ion from a carbonyl compound, the energy of the LUMO (lowest unoccupied molecular orbital) is lowered, the α -CH-acidity increases and nucleophilic additions such as pericyclic reactions and conjugate additions are facilitated (Figure 18). The first examples of enantioselective iminium catalysis were reported by the group of MacMillan in 2000, where they developed Diels-Alder reactions, 1,3-dipolar cycloadditions and conjugate additions of electron rich heteroaromatic as well as aromatic compounds, catalyzed by an imidazolidinone catalyst, which can be derived from chiral amino acids.²¹

Figure 18: General scheme of iminium catalysis.²¹

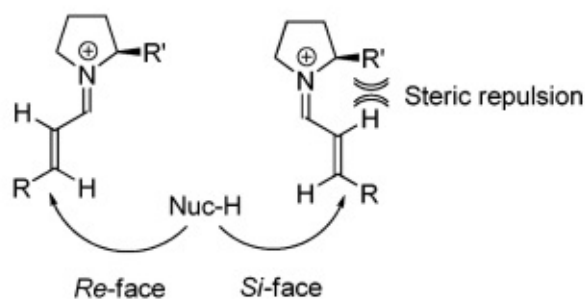
A collection of successfully used catalysts for iminium catalysis can be found in Figure 19.

Figure 19: Collection of catalysts used for iminium catalysis.²⁰

The mechanism of the β -functionalization of α,β -unsaturated substrates via iminium catalysis is similar to the enamine activation (Figure 20). The catalytic cycle starts again with the condensation of the secondary amine catalyst and the α,β -unsaturated carbonyl compound, giving an iminium ion. Nucleophilic addition to the β -carbon of the reactive iminium intermediate gives the β -functionalized enamine. This enamine is in tautomeric equilibrium with its corresponding iminium ion and hydrolyzation releases the product and the catalyst can reenter the catalytic cycle, similarly to the enamine catalysis.¹⁹

Figure 20: Catalytic cycle of the iminium activation.²¹

The reactivity and the structure of the iminium-ion intermediate have been studied and contrary to the α -functionalizations via enamine catalysis where the directing effects of the electrophile can be either through H-bonding or steric interactions, in iminium catalysis the direction of the nucleophile relies mainly on steric hindrance that shields one side of the intermediate (Figure 21).¹⁹

Figure 21: Influence of steric interactions in the pyrrolidine catalyzed β -functionalization of α - β -unsaturated aldehydes.¹⁹

The concept of iminium catalysis has also been outstretched to other highly enantioselective reactions, such as epoxidations, cyclopropanations and conjugate reductions, as well as Michael additions of malonates and nitroalkanes to enones, Mukaiyama-Michael reactions, Friedel-Crafts alkylations with pyrroles, indoles and benzenes and cycloadditions with nitrones.^{18, 21}

1.2.3 Iminium-enamine tandem catalysis

Enamine and iminium catalysis represent two different activation modes in organocatalysis, since in enamine catalysis the carbonyl substrate is transformed into a more nucleophilic enam-

ine, which results in the increase of the HOMO energy. On the other hand, in iminium catalysis the activation of the carbonyl substrate is promoted by the lowering of the energy of the LUMO via the iminium-ion formation, making the intermediate more electrophilic. Nevertheless, enamine catalysis works via iminium-ion formation and iminium catalysis results in the formation of an enamine intermediate. Because of this coherence, the combination of these two organocatalytic disciplines is very attractive.²¹ Iminium-enamine tandem reactions all have in common that they need enal or enone systems as substrates. Activation of the substrate with an amine catalyst results in the formation of an iminium-ion intermediate (Figure 22). After the nucleophilic conjugate addition, an enamine intermediate is formed, which can now react with an electrophile to give the double-substituted product, that contains two new stereocenters.²²

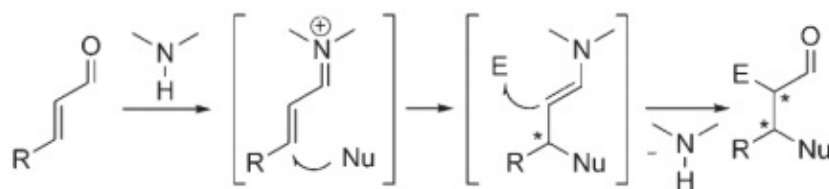


Figure 22: General scheme of the iminium-enamine activation.²²

An example of such an iminium-enamine tandem reaction is the enantioselective α -halogenation of 2-methylfuran (Figure 23), reported by MacMillan, using imidazolidinone-based catalysts (Figure 24). These reactions show high enantioselectivity and are an attractive option for the synthesis of complex molecules in a simple one-flask reaction.²³

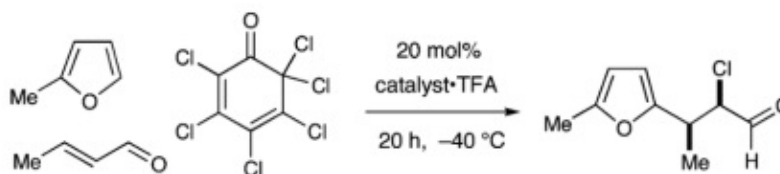


Figure 23: Example for an α -halogenation reaction.²³

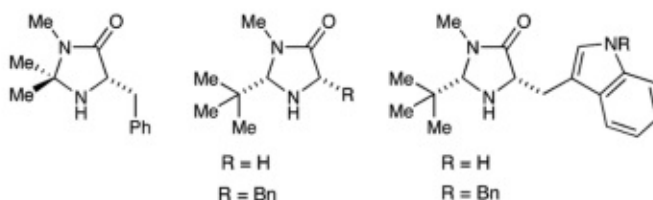


Figure 24: Imidazolidinone catalysts used by MacMillan.²³

1.2.4 Singly occupied molecular orbital catalysis

The third method in covalent amine catalysis is the singly occupied molecular orbital (SOMO) activation. Through a one-electron oxidation of an enamine intermediate with a metal salt as oxidant, a 3- π -electron SOMO activated species is formed (Figure 25). This generated reactive radical cation can react with a wide range of nucleophilic SOMOphiles due to its electrophilicity at the α -carbon of the enamine.^{24, 25, 13}

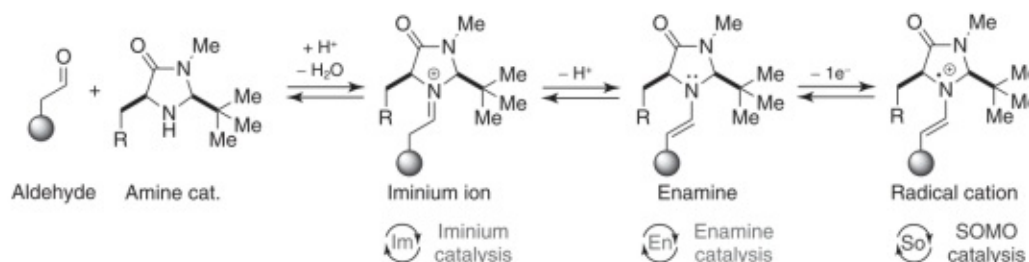
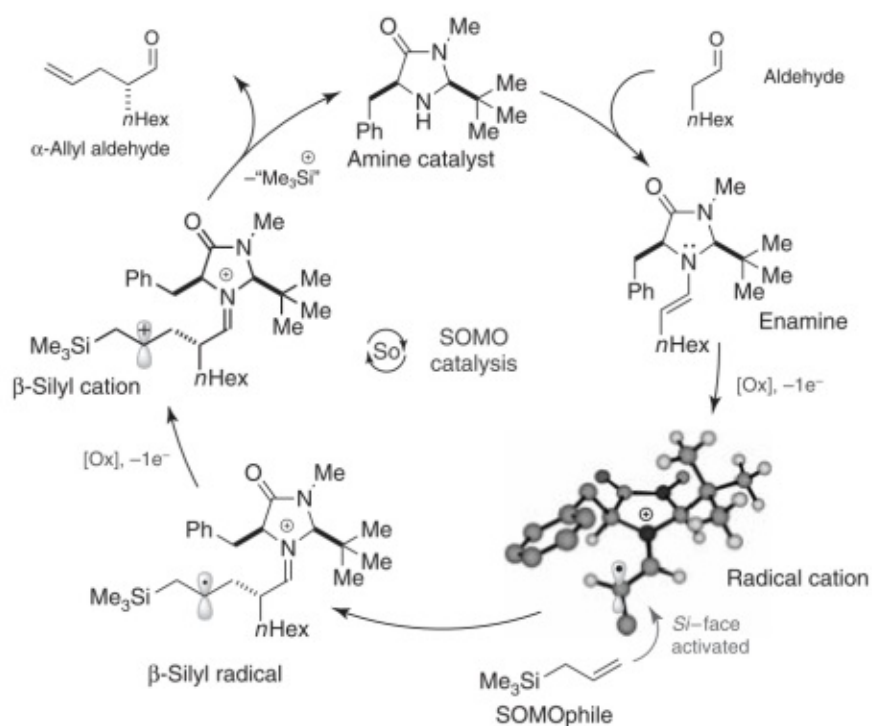


Figure 25: Overview of the activation modes in amine catalysis.²⁵

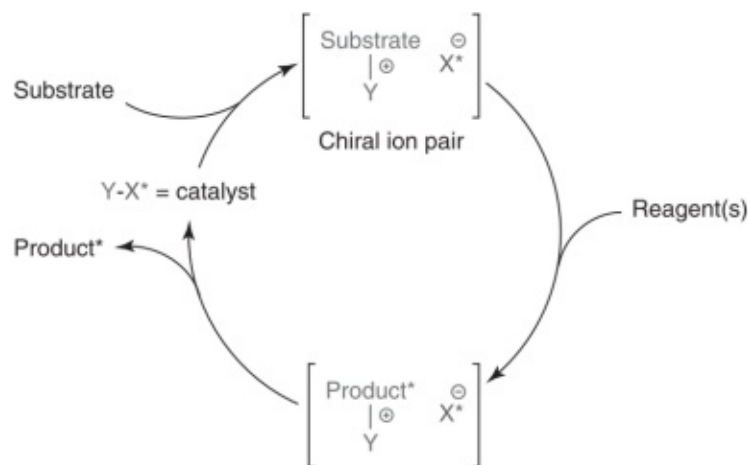
The SOMO catalysis was first described by the group of MacMillan, as the limitations of enamine catalysis in the α -alkylation of aldehydes and ketones raised their interest.²⁵ So far, approaches to the asymmetric organocatalytic α -alkylation have been hindered through the *N*-alkylation of the catalyst. To avoid this problem, the reactivity of the alkylation reagent, the catalyst and the aldehyde must be geared to each other.¹⁹ The group of MacMillan has then found out that the SOMO activation opens up a new strategy to solve this problem.

An example for SOMO catalysis is shown in Figure 26. The imidazolidinone catalyst first condenses with the aldehyde substrate to form an enamine. This enamine intermediate is selectively oxidized by a metal salt oxidant, in this example CAN (ceric(IV) ammonium nitrate), to give the crucial 3- π -electron radical cation. This radical intermediate can now undergo an enantioselective C-C-bond formation with the here used allylsilane as the SOMOphile and forms the β -silyl radical. After a second single-electron transfer (SET) with the oxidant, a stabilized β -silyl cation can be formed and β -silyl elimination as well as hydrolysis of the iminium ion gives the desired product and the regenerated imidazolidinone catalyst.²⁵

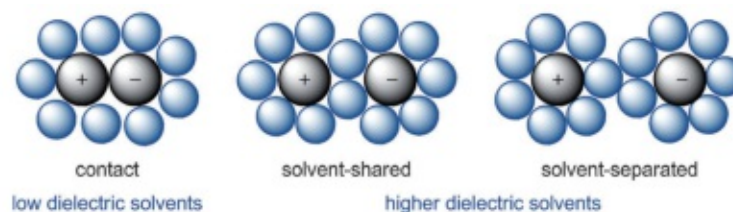
Figure 26: Catalytic cycle of SOMO catalysis.²⁵

1.2.5 Asymmetric counteranion directed catalysis

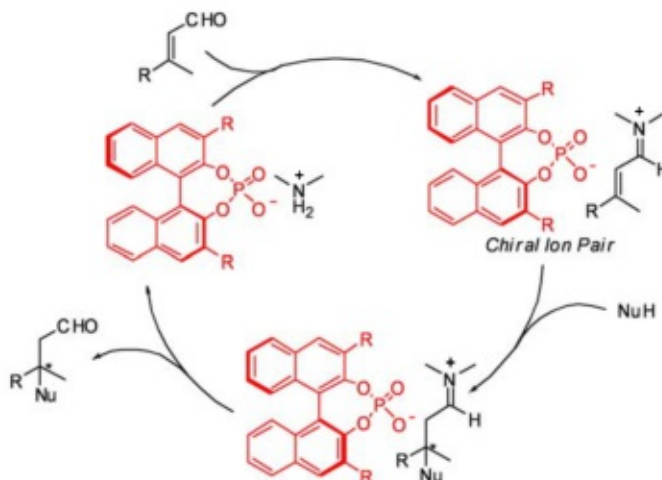
The concept of asymmetric counteranion directed catalysis (ACDC) describes a reaction with a cationic intermediate where the enantioselectivity gets induced via ion pairing with an enantiomerically pure, chiral anion (Figure 27).²⁶

Figure 27: General principle of ACDC.²⁷

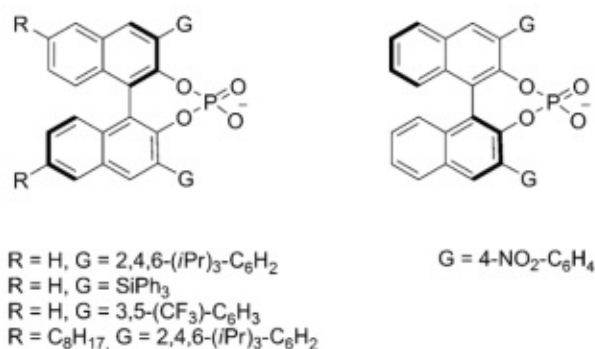
Every reaction that involves a charged intermediate or transition state is accompanied by a counterion as a result of the electroneutrality principle. If the ion pairs are not separated due to solvent effects, the counterion can influence the enantioselectivity of the reaction.²⁸ In Figure 28, the three different types of ion pairs are shown. Ion pairs that have their own solvation shell are called solvent-separated ion pairs and solvent-shared ion pairs share a solvation shell. Apart from that, there are also contact ion pairs which do not have solvent molecules between them and share one solvation shell. Such contact ion pairs are generally favored in nonpolar solvents with low dielectric constants and show a bigger influence on their environment. As a result, higher selectivities are observed in nonpolar solvents for reactions where ion pairing interactions play a crucial role in selectivity control.²⁹

Figure 28: Different types of ion pairs.²⁹

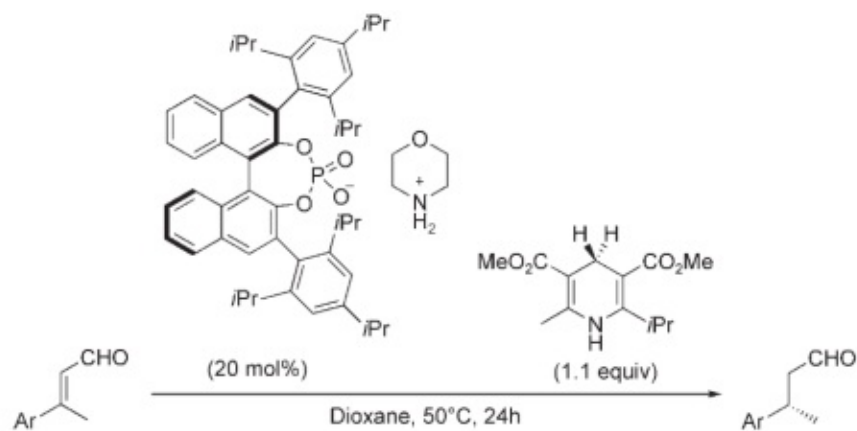
In iminium catalysis, a strong influence of the counteranion regarding enantioselectivity and yield could be observed (Figure 29). Commonly used catalytic salts in ACDC catalysis consist of an achiral amine and a chiral phosphoric acid derivative.¹¹

Figure 29: ACDC in iminium catalysis.¹¹

Especially BINOL-derived monophosphoric acids showed very attractive properties for hydrogen-bond catalysis. On the other hand, for reactions using ion pairs, the conjugate bases of such BINOL-derived phosphoric acids occupied an important place as powerful counterions (Figure 30).²⁹

Figure 30: Examples of BINOL-derived phosphoric acid counteranions.²⁹

The research groups of List and MacMillan have both independently reported the use of ACDC catalysis for a metal-free asymmetric transfer-hydrogenation of α - β -unsaturated aldehydes. The reaction uses a Hantzsch dihydropyridine as the reductant and a catalyst salt consisting of an achiral ammonium cation and a chiral BINOL-derived phosphate anion (Figure 31). Due to the strong counteranion effect, a positive influence of the phosphoric acid anion on yield and enantioselectivity could be observed. The best results were observed using the derived sterically-hindered chiral phosphoric acid 3,3'-bis(2,4,6-triisopropylphenyl)-1,1'-binaphthyl-2,2'-diyl hydrogen phosphate (TRIP), and morpholine as the catalyst salt. Using this catalyst salt, a wide range of substrates could be obtained in high yields and enantioselectivities between

98:2 and >99:1 e.r.³⁰Figure 31: ACDC-mediated transfer hydrogenation of α - β -unsaturated aldehydes.³⁰

1.3 Counterion enhanced organocatalysis

The group of Schröder has recently reported a new organocatalytic concept, the counterion enhanced organocatalysis which has already been successfully applied to the asymmetric transfer hydrogenation of enones (Figure 32).³¹

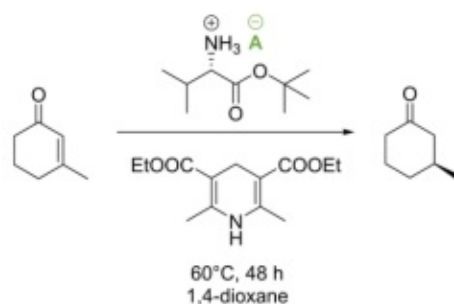


Figure 32: Counterion enhanced organocatalytic asymmetric transfer hydrogenation using Hantzsch ethyl ester as reductant.³¹

In the past years, two groups of catalyst systems have proved to be very effective for the asymmetric transfer hydrogenation. On the one hand, there are the imidazolidinone derivatives, used by the group of MacMillan, for highly enantioselective conjugate hydrogenations of α,β -unsaturated aldehydes and ketones.³² On the other hand, the group of List achieved excellent results in the hydrogenation of enals and enones using ACDC catalysis with a catalyst salt consisting of an ammonium cation and TRIP, a sterically-demanding and enantiopure phosphate anion (Figure 33).³⁰

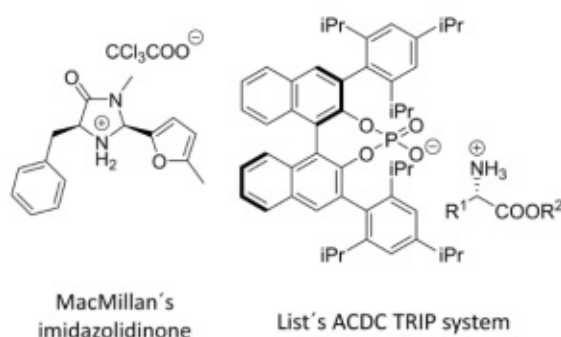


Figure 33: MacMillan's and List's catalyst systems for the asymmetric transfer hydrogenation.³¹

Nevertheless, these two catalytic strategies do have some limitations. While MacMillan's catalyst works very well for enals, higher catalyst loadings are needed for enones due to a lower reactivity. List's catalyst system gives excellent results for both, enals and enones, even with a low catalyst loading. Still, the catalyst is quite expensive and a five-step synthesis with rather

low overall yields is needed.³¹ These limitations led to the idea of a straightforward, cheaper and chiral-pool derived catalytic system, which combines both, a high catalytic activity and an excellent enantioselectivity. As a result, the group of Schröder proposed the novel concept of counterion enhanced organocatalysis using a chiral amino acid cation, which is easily accessible, cheap and chiral-pool derived, as well as a C₂-symmetric achiral or racemic phosphate anion (Figure 34), which although not enantiomerically pure still shows a positive effect on the enantioselectivity. Similarly to the amino acid cation, the phosphate anion is easily accessible and cheap. Using this novel catalyst system the reduction of α,β -unsaturated ketones could be carried out with high yields and selectivities.³¹

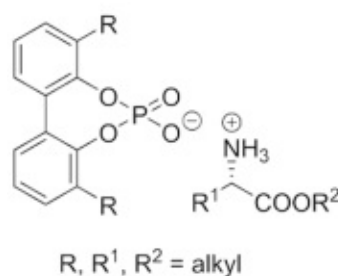


Figure 34: Catalyst system for the counterion enhanced organocatalysis.³¹

Recently, this concept of counterion enhanced organocatalysis has also been successfully applied in a direct asymmetric α -allylation of branched aldehydes (Figure 35) using a Pd-source together with a chiral amine and an achiral or racemic phosphoric acid³³, as well as in the asymmetric epoxidation of enones.

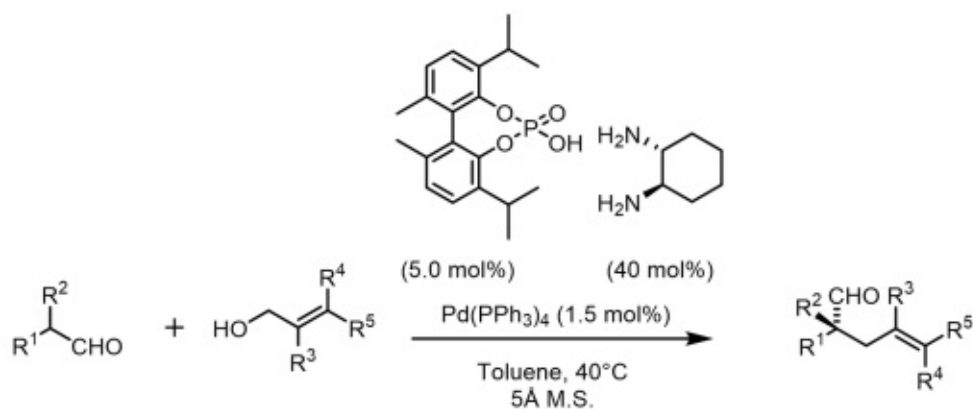


Figure 35: Asymmetric α -allylation of α -branched aldehydes.³³

2 State of the art

The general scheme and the state-of-the-art catalytic system for the asymmetric aziridination of cyclic enones, which has been developed by the group of Melchiorre, are shown in Figure 36 and Figure 37, respectively. The state-of-the-art approach employs a 9-amino(9-deoxy)*epi*-hydroquinine (9-*epi*-NH₂-HQ), a Cinchona-derived primary amine and a Boc-protected amino acid. The reaction is generally carried out at room temperature and uses a protected and tosylated hydroxylamine as the reactant, giving the aziridine products with high enantioselectivities and good yields.³⁴ The state-of-the-art Cinchona-based catalysts are easily available and already known as organocatalysts. However, they show one big disadvantage, which is their limited options for modification.

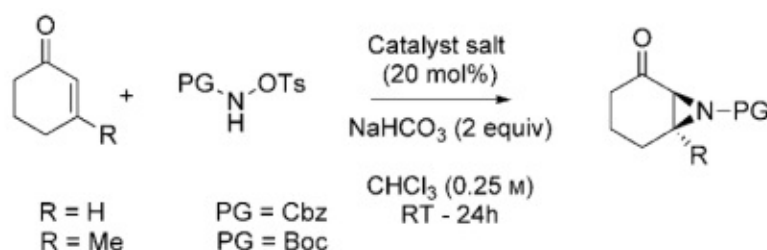


Figure 36: General scheme for the asymmetric aziridination of cyclic enones.³⁴

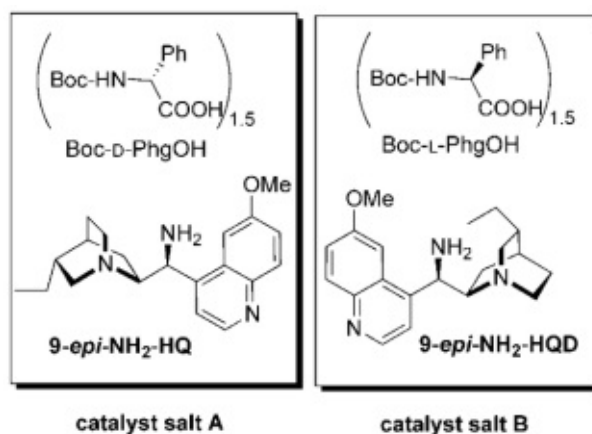


Figure 37: State-of-the-art catalyst systems for the asymmetric aziridination.³⁴

3 Aim of the thesis

Since the aziridine scaffold is part of several drug candidates and biologically active molecules as well as bulk chemicals, its synthesis is of great interest, not only for pharmaceutical purposes.^{1,4} Due to the growing importance of these molecules, several synthetic methods have been developed, however, most of them in the field of transition-metal catalysis. Only recently, organocatalytic methods for the asymmetric aziridination have been reported, which can be ascribed to the recently growing interest and importance of organocatalysis in general.

The state-of-the-art catalytic system used for the asymmetric aziridination of cyclic enones uses a Cinchona-derived primary amine and a Boc-protected amino acid, as can be seen in Figure 37. This catalyst system has already been used as organocatalyst for other reactions and is generally easily available. Nevertheless, the limited modification possibilities display a big drawback of such Cinchona-based catalysts.

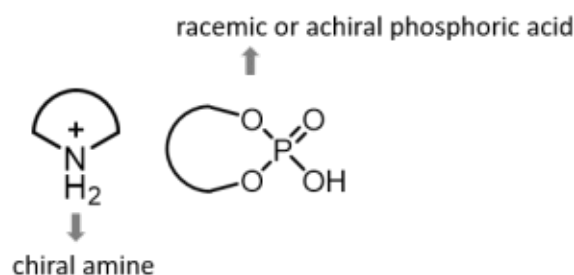


Figure 38: General catalyst scheme for the asymmetric counterion enhanced organocatalytic aziridination.

In this thesis, an alternative catalyst system for the asymmetric aziridination of cyclic enones, using the concept of counterion enhanced organocatalysis, was evaluated. The new catalyst system should consist of a chiral amine, obtained from an amino acid from the chiral pool, and an achiral or racemic phosphoric acid as the counterion, which still has an influence on the enantioselectivity (Figure 38). Generally, the two catalyst components should be easy to prepare by using cheap precursors. Furthermore, modification should be easy, in contrast to the state-of-the-art catalyst. The catalyst system as well as the reaction conditions should be optimized and lastly the scope of the reaction investigated.

4 Results and discussion

4.1 Catalyst optimization

At the beginning, the catalyst components for the asymmetric aziridination were optimized using literature conditions.³⁴ Cyclohex-2-en-1-one was used as the substrate and *tert*-butyl (tosyloxy)carbamate **3** was the reactant (Figure 39). The reaction was carried out at room temperature, in chloroform and with 2 equiv. of base. As a first step, the amine-functionality as well as the phosphoric acid of the catalyst system was optimized.

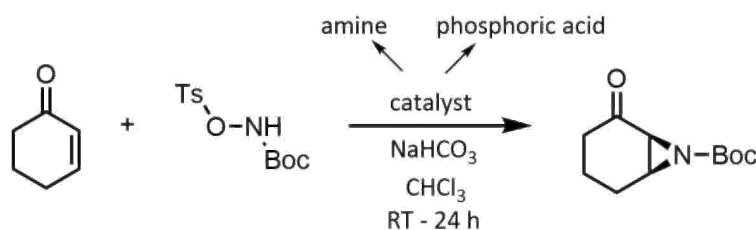


Figure 39: General reaction scheme for the catalyst optimization.

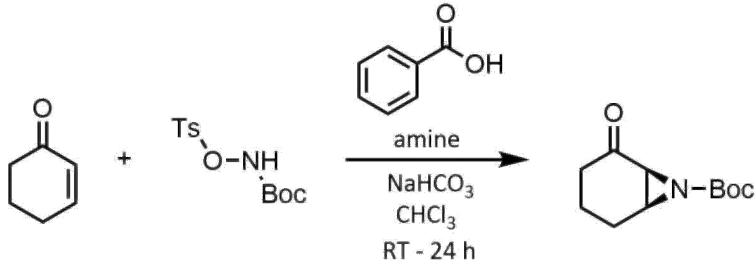
4.1.1 Screening of the amine-functionality

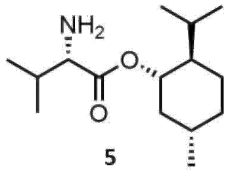
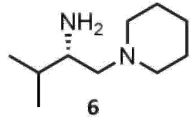
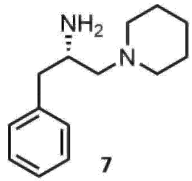
In terms of the screening of the amine-functionality, there were two questions to answer. The first was, whether we do need a diamine or a sterically demanding ester, which was used for the asymmetric transfer-hydrogenation in section 1.3. In case a diamine is needed, the next question was if then an aliphatic or an aromatic diamine would work better. The results of this first amine screening are shown in Table 2.

At first the L-valine-menthyl ester **5** (entry 1) was tried, since it gave the best results in the asymmetric transfer-hydrogenation.³¹ Nevertheless it gave only the racemic product and therefore no conversion was determined. Due to the fact that a sterically-demanding ester did not work for the asymmetric aziridination, diamines were tested next. Therefore we started with an aliphatic diamine **6** (entry 2) which gave a moderate conversion and a good enantioselectivity. For the aromatic diamine **7** (entry 3) the same enantioselectivity but a significantly better conversion could be observed compared to the aliphatic diamine. This led to the conclusion that an aromatic diamine is necessary to achieve both, good enantioselectivities and conversions. At this point, no further diamines have been tested, since the question about which kind of amine is needed could be answered and a broader range of aromatic amines have been tested

later on in a bigger catalyst screening.

Table 2: Optimization of the amine-functionality.



entry ^[a]	amine	acid equiv.	conv. [%] ^[b]	ee [%] ^[c]
1		1	n.d.	racemic
2		1.5	56	72
3		1.5	97	72

^[a] Reaction carried out using 0.25 mmol ketone, 10 mol% catalyst and 0.21 mmol reactant in 0.8 ml solvent for 24 h at room temperature.

^[b] Determined via GC-MS.

^[c] Determined via chiral HPLC.

The fact that the reaction with the sterically-demanding ester did only give the racemic product, showed that the reaction does not rely on steric interactions as it is the case in the asymmetric transfer-hydrogenation³¹, and leads to the assumption that hydrogen-bonding interactions between the tertiary amine of the catalyst and the hydrogen atom of the hydroxylamine reactant are necessary (Figure 40). These hydrogen-bonding interactions influence the direction from which the reactant is inserted into the double bond and therefore, have an influence on the enantioselectivity.

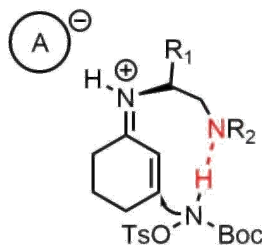
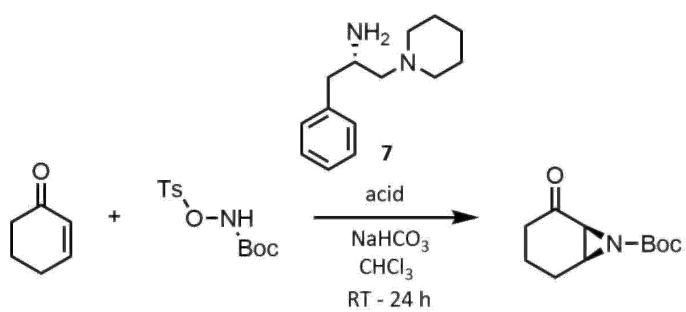


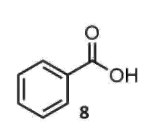
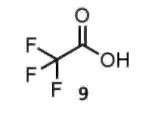
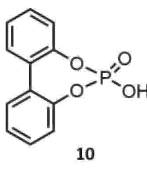
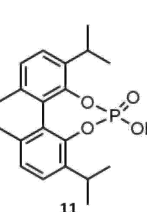
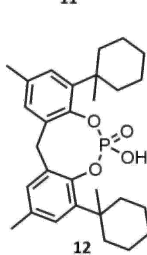
Figure 40: Proposed hydrogen-bonding interactions between the catalyst and the reactant.

4.1.2 Screening of the phosphoric acid anion

Knowing that we need an aromatic diamine as the amine component of the catalyst, the next step was to find out what kind of phosphoric acid was needed. Therefore, three different phosphoric acids (Table 3, entries 3 to 5) were evaluated. The best results, concerning both conversion and ee, could be observed using the aromatic diamine **7** and the unsubstituted phosphoric acid **10** (entry 3). The phosphoric acid **12** (entry 5) gave an even slightly better ee, however, the conversion was significantly lower and phosphoric acid **11** (entry 4) gave rather low conversion and moderate enantioselectivity. Using benzoic acid **8** (entry 1), as in the screening of the amine-functionality, gave similar results. TFA **9** (entry 2) was also tested, which gave only the racemic product.

Table 3: Optimization of the acid-derived anion.



entry ^[a]	acid	acid equiv.	conv. [%] ^[b]	ee [%] ^[c]
1		1.5	97	72
2		1.5	n.d.	racemic
3		1.5	91	73
4		1.5	21	66
5		1.5	53	74

^[a] Reaction carried out using 0.25 mmol ketone, 10 mol% catalyst and 0.21 mmol reactant in 0.8 ml solvent for 24 h at room temperature.

^[b] Determined via GC-MS.

^[c] Determined via chiral HPLC.

Based on the results of the first screenings, the catalyst system using diamine **7** and phosphoric acid **10** (Table 3, entry 3) was initially selected for further optimization. Since a phosphoric acid which gives moderate enantioselectivities and good conversions was selected, the question was, what amount of this acid would be required. Hence, the asymmetric aziridination has been carried out using different acid equivalents of the phosphoric acid **10**. More precisely 1, 1.5 and 2 equivalents of the acid were tested (Figure 41). As a result, it could be shown that 1 equivalent of the phosphoric acid gave the highest conversion with constant enantioselectivity and therefore, from this point on, 1 equivalent of the acid was used for all the reactions.

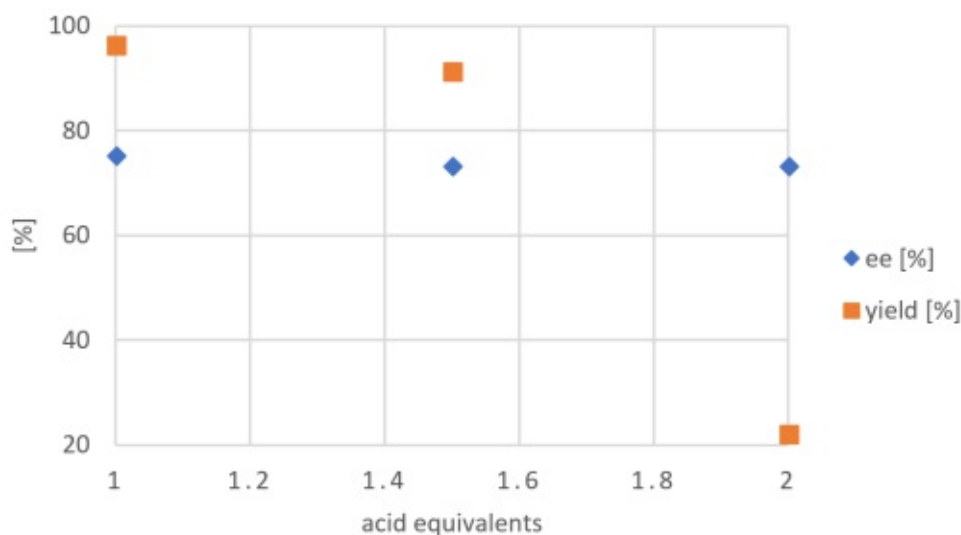


Figure 41: Acid equivalents screening.

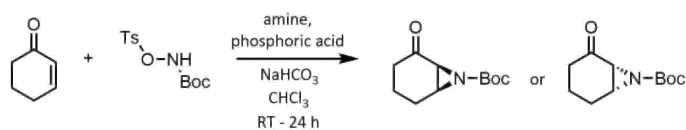
4.1.3 Catalyst screening

The final step, in terms of catalyst optimization, was to screen different combinations of aromatic diamines and phosphoric acids in order to find the catalyst system which yields the optimum results. The results obtained with the catalysts screened can be seen in Table 4 and Table 5. Starting with Table 4, for entries 1 to 6, the D-phenylglycine-based diamine **22**, was used as the amine source and different phosphoric acids were screened. With the biphenyl phosphoric acid **10** (entry 1), only rather low conversion and moderate enantioselectivity could be observed. For entries 2 to 6 in Table 4, phosphoric acids **29**, **33**, **34**, **35** and **36** were tested. All of these catalysts gave excellent conversions and good enantioselectivities. Especially with the catalyst using diamine **22** and the phosphoric acid **33** (entry 3), an excellent enantioselectivity could be achieved as well. Entries 7 and 8 in Table 4 use the L-phenylglycine-based diamine **25**, as the amine source and the two different phosphoric acids **33** and **12**. While moderate

conversion and enantioselectivity could be observed with the phosphoric acid **33** (entry 7), only low conversion and moderate enantioselectivity could be achieved with the acid **12** (entry 8). Continuing with Table 5, entries 9 and 10 use the L-phenylalanine-based diamine **7** and the two different phosphoric acids **37** and **33**, giving moderate results for both catalysts. Also for the combination of the L-phenylalanine-based diamine **26**, together with the phosphoric acid **33** (entry 10), as well as the catalyst using diamine **27** and the phosphoric acid **12** (entry 11), the results could not exceed a moderate range. Entries 12 and 13 use the tryptophane-based diamine **28** and with the phosphoric acid **10** (entry 12) excellent conversion could be obtained, however, the enantioselectivity was rather low. Also with the best performing phosphoric acid **33** (entry 13) the results were sobering.

To sum up, the best conversion and enantioselectivity was observed with the catalyst using the diamine **22**, together with the phosphoric acid **33** (Table 4, entry 3), giving 98% conversion and 98% ee. Therefore, this catalyst system was used for all further reactions and optimizations.

Table 4: Catalyst screening 1.



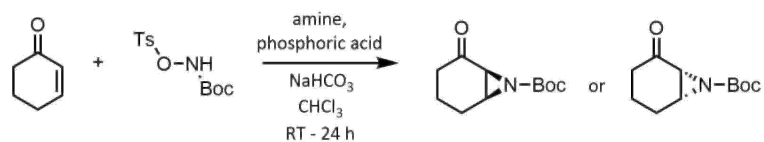
entry ^[a]	amine	acid	conv. [%] ^[b]	ee [%] ^[c]
1			28	60
2			94	90
3			98	98
4			99	85
5			99	87
6			98	87
7			64	81
8			6	60

^[a] Reaction carried out using 0.25 mmol ketone, 10 mol% catalyst and 0.21 mmol reactant in 0.8 ml solvent for 24 h at room temperature.

^[b] Determined via GC-MS.

^[c] Determined via chiral HPLC.

Table 5: Catalyst screening 2.



entry ^[a]	amine	acid	conv. [%] ^[b]	ee [%] ^[c]
9			99	68
10			86	66
11			72	66
12			64	57
13			99	56
14			59	49

^[a] Reaction carried out using 0.25 mmol ketone, 10 mol% catalyst and 0.21 mmol reactant in 0.8 ml solvent for 24 h at room temperature.

^[b] Determined via GC-MS.

^[c] Determined via chiral HPLC.

4.2 Optimization of the reaction conditions

In order to optimize the reaction conditions, different bases, base equivalents as well as solvents were screened. As catalyst for this optimization, the catalyst system shown in Figure 42 was chosen, since it demonstrated the best performance in the previous catalyst optimizations (section 4.1).

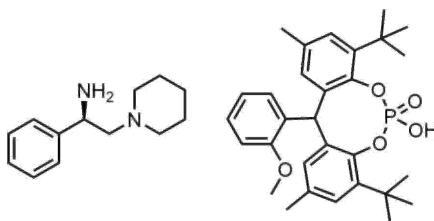
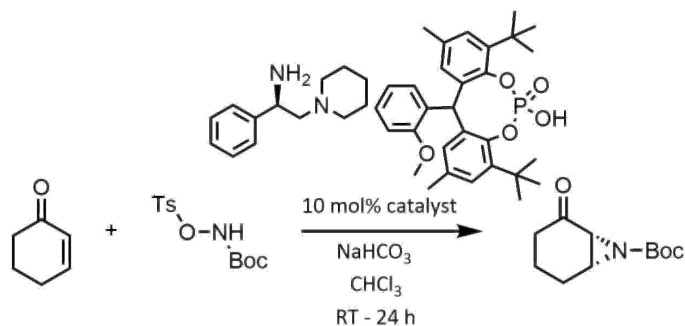


Figure 42: Optimized catalyst system.

4.2.1 Optimization of the base and base equivalents

The reaction was first carried out using NaHCO_3 as the base, in analogy to the literature.³⁴ Therefore, we screened different base equivalents, as can be seen in entries 1 to 3, in Table 6. 2 and 1 equivalents of NaHCO_3 as well as no NaHCO_3 were used and the best results were obtained with 2 equivalents of base (entry 3), while 1 equivalent yielded worse results and the reaction did not work at all in the absence of a base. After the base equivalents were fixed, additional bases were tested, shown in entries 4 to 8, in Table 6. Nevertheless, the reaction did not work using an organic base like diisopropylethylamine or lutidine (entries 5 and 7). With Na_2CO_3 and pyridine the reaction succeeded (entries 4 and 6), however, only the racemic product was obtained with Na_2CO_3 and the reaction with pyridine just gave moderate enantioselectivity. Using Cs_2CO_3 (entry 8) only minor conversion could be observed. As a result, the aziridination was further carried out using 2 equivalents of NaHCO_3 .

Table 6: Base and base equivalents screening.



entry ^[a]	base	equiv.	solvent	conv. [%] ^[b]	ee [%] ^[c]
1	NaHCO ₃	0	Chloroform	n.d.	n.d.
2	NaHCO ₃	1	Chloroform	36	57
3	NaHCO ₃	2	Chloroform	98	98
4	Na ₂ CO ₃	2	Chloroform	25	n.d.
5	Diisopropylethylamine	2	Chloroform	n.d.	n.d.
6	Pyridine	2	Chloroform	23	68
7	Lutidine	2	Chloroform	n.d.	n.d.
8	Cs ₂ CO ₃	2	Chloroform	5	n.d.

^[a] Reaction carried out using 0.25 mmol ketone, 10 mol% catalyst and 0.21 mmol reactant in 0.8 ml solvent for 24 h at room temperature.

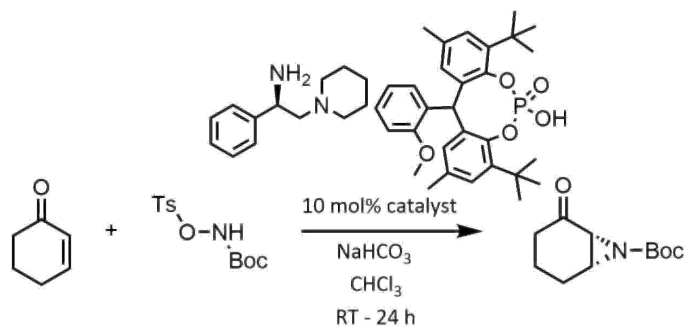
^[b] Determined via GC-MS.

^[c] Determined via chiral HPLC.

4.2.2 Optimization of the solvent

In addition to chloroform, different solvents were tested. As can be seen in Table 7, the reaction using dioxane and methyl *tert*-butyl ether (MTBE) (entries 2 and 3) gave poor results and no enantiomeric excess could be determined. Using dichloromethane (DCM) as the solvent led to a very high conversion, however, the respective enantioselectivity was only moderate (entry 4). In contrast to chloroform (entry 1), which gives both high enantioselectivity and conversion, the other solvents that were evaluated could not exceed its performance.

Table 7: Solvent screening.



entry ^[a]	base	equiv.	solvent	conv. [%] ^[b]	ee [%] ^[c]
1	NaHCO ₃	2	Chloroform	98	98
2	NaHCO ₃	2	Dioxane	11	n.d.
3	NaHCO ₃	2	MTBE	7	n.d.
4	NaHCO ₃	2	DCM	99	64

^[a] Reaction carried out using 0.25 mmol ketone, 10 mol% catalyst and 0.21 mmol reactant in 0.8 ml solvent for 24 h at room temperature.

^[b] Determined via GC-MS.

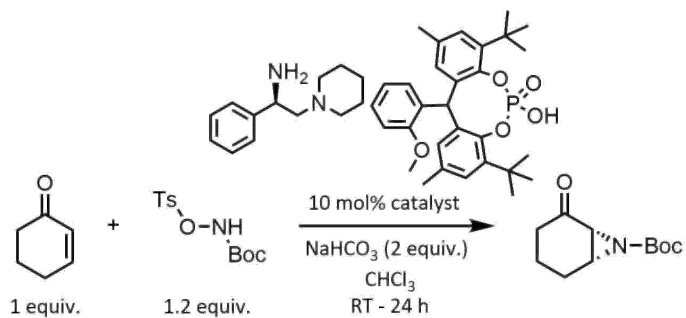
^[c] Determined via chiral HPLC.

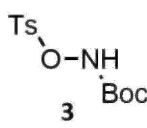
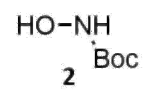
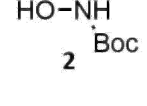
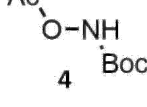
Based on the results that were obtained through these optimization steps, the best reaction conditions turned out to be chloroform as the solvent and 2 equivalents of NaHCO₃ as the base.

4.3 Reactant optimization

While excellent results could be achieved by using the tosylated Boc-protected hydroxyl-amine **3** (Table 8, entry 1), the performance of two other reactants **2** and **4** was also evaluated. However, as can be seen in Table 8, the results using only the Boc-protected hydroxylamine **2** as well as the acetylated Boc-protected hydroxylamine **4** were disappointing. Considering entries 2 and 3, the reaction was carried out using the Boc-protected hydroxylamine **2** as the reactant, once with base and once without base. Nevertheless, in both cases, the desired aziridine product could not be detected. In entry 4, the acetylated Boc-protected hydroxylamine **4** was used. With this reactant, the desired product could be obtained, but with a significantly lower enantioselectivity and numerous side products. These results led to the conclusion that the tosylated Boc-protected hydroxylamine **3** is indeed necessary as the reactant, in order to achieve high selectivity, since the tosyl-group is a better leaving group.

Table 8: Optimization of the reactant.



entry ^[a]	reactant	base	conv. [%]	ee [%] ^[b]
1		NaHCO ₃	98 ^[c]	98
2		NaHCO ₃	n.d.	n.d.
3		-	n.d.	n.d.
4		NaHCO ₃	trace	63

^[a] Reaction carried out using 0.21 mmol ketone, 10 mol% catalyst and 0.25 mmol reactant in 0.8 ml solvent for 24 h at room temperature.

^[b] Determined via chiral HPLC.

^[c] Determined via NMR.

4.4 Catalyst synthesis

The developed catalyst system for the asymmetric aziridination consists of the diamine and the phosphoric acid, as shown in Figure 43. Considering the synthesis of these catalyst components, we aimed to develop suitable synthetic pathways for both components that are short and easy to carry out. Furthermore, we considered inexpensive and commercially available precursors.

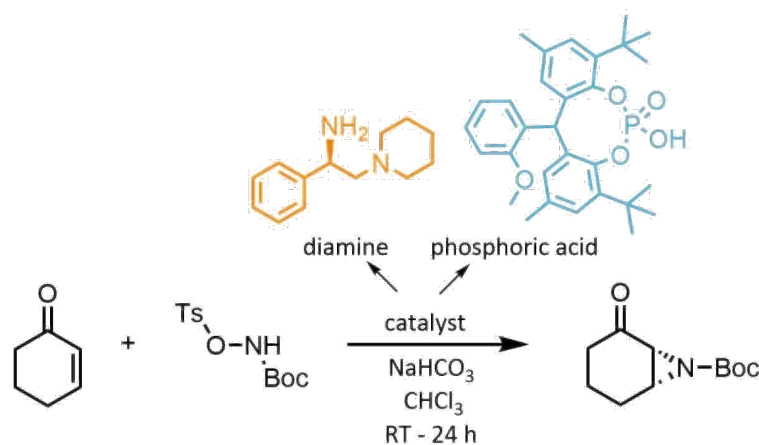


Figure 43: Catalyst components used for the asymmetric aziridination of cyclic enones.

4.4.1 Diamine synthesis

The reaction scheme for the diamine synthesis from D-phenylglycine **15** is shown in Figure 44 and it was carried out the same way with L-phenylglycine **17**. Considering the starting materials, the amino acids D- and L-phenylglycine were used, since they can be obtained from the chiral pool, are cheap and commercially available. The first step, is a Boc-protection of the amine function of the amino acid using Boc₂O in THF and the protected product **16** can be obtained with a nearly quantitative yield.³⁵ The next step, is a coupling reaction of the acid group of the amino acid and piperidine, giving product **19**. The coupling is done using DCC as the coupling reagent and oxyma **14**, which is the oxime of the ethyl cyanoacetate, as additive in DCM.³⁶ Through the oxyma, an activated ester is formed and as a result, unwanted side reactions can be suppressed, furnishing the product in good yields, comparable with the commercially available 1-hydroxybenzotriazole (HOBT). After the coupling, the deprotection of the amine function is performed with acetylchloride in methanol, in order to get the primary amine salt **21** in high yields.³⁶ The final step of the diamine synthesis, is the reduction of the carbonyl group. Therefore, LiAlH₄ in THF is used to obtain the desired diamine compound **22**,³⁷ however, only in moderate yields. Nevertheless, over all the entire synthetic process can be performed in

four steps and all the single reactions are easy and convenient to carry out, since no special arrangements need to be made. Another noteworthy advantage is the good availability of the starting material from the chiral pool as well as the low price. All things considered, with this synthetic pathway, the criteria for a cheap and easy synthesis for the diamine can be fulfilled.

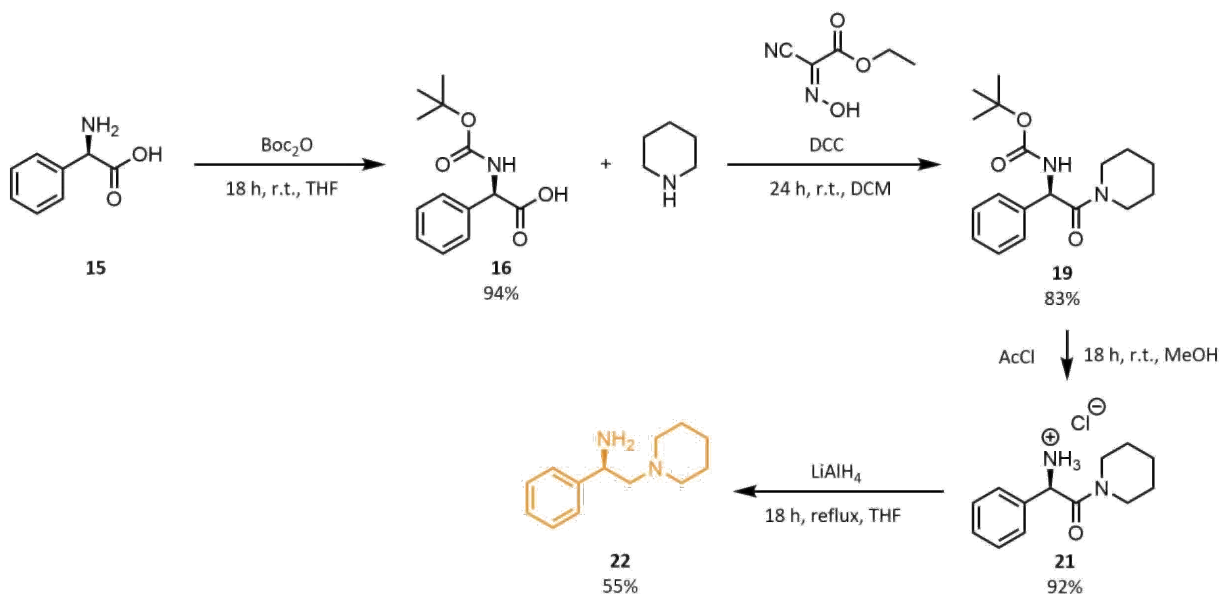


Figure 44: Reaction scheme of the diamine synthesis.

4.4.2 Phosphoric acid synthesis

The synthesis of the phosphoric acid could be done in two steps and the appropriate reaction scheme can be seen in Figure 45. The first step is a Friedel-Crafts type reaction, where the aldehyde **31** gets activated by protonation, followed by the electrophilic attack of the electron rich phenol **30**. Then, a second phenol molecule is added and after cleavage of water, the intermediate product **32** is obtained in moderate yield.³⁸ The phosphoric acid formation from this intermediate is achieved by first, using phosphoryl chloride (POCl_3), followed by hydrolysis with $\text{H}_2\text{O}/\text{HCl}$.³⁹ The desired phosphoric acid **33** could consequently be obtained with excellent yield. Overall, also the phosphoric acid synthesis is easy, in terms of preparation, and the starting materials are cheap and easily available, making it a cost-efficient and easy to carry out synthetic route which is also suitable for up-scaling.

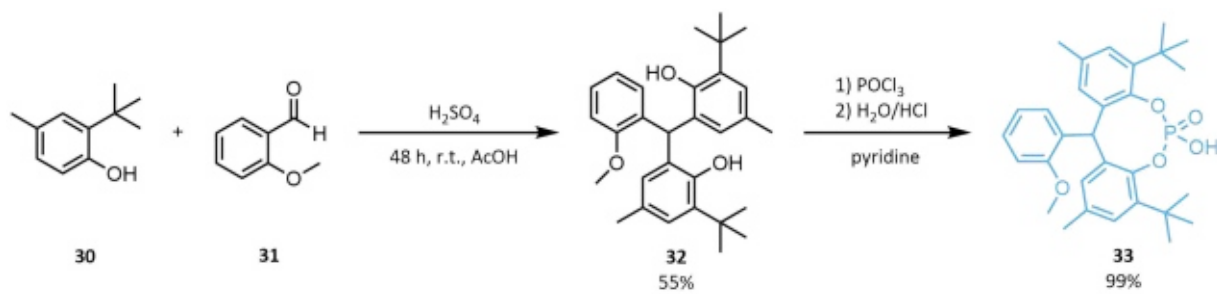


Figure 45: Reaction scheme of the phosphoric acid synthesis.

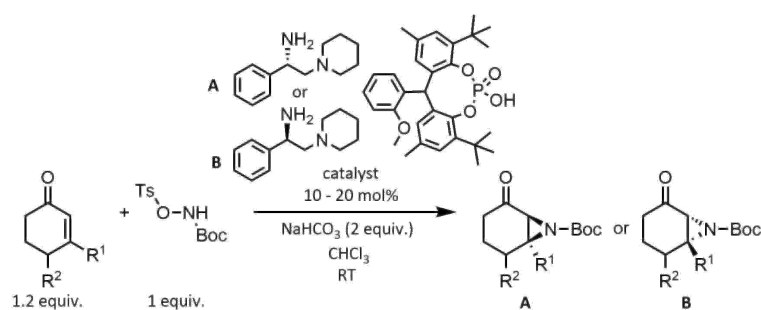
4.5 Substrate scope and limitations

After determining the best catalyst system (section 4.1) and optimizing the reaction conditions (section 4.2), the reaction was carried out with a few more substrates. The substrates as well as the respective results can be seen in Table 9. The catalytic reactions have been performed with both enantiomers of the diamine, marked with A and B, giving the two enantiomeric products, which are also marked with A and B. As shown in Table 9, good ee and good yield could be achieved with substrates **38** to **41**.

Nevertheless, satisfying results were not obtained with all the tested substrates. 3-Phenyl-cyclohexenone **42** (entry 5) showed no reactivity, probably due to the conjugated ring system. For the 3-methyl-cyclopentenon **43** (entry 6) only a very low conversion could be observed, which leads to the conclusion, that cyclopentenones are significantly less reactive than the cyclohexenones, because of their different ring properties. Even though the 3-hexyl-cyclohexenone **44** (entry 7) gave good enantioselectivity, the conversion was rather low, even after a very long reaction time (120 h). Steric hindrance of the hexyl group can be a possible explanation for this low conversion. In order to obtain good results also with the substrates that initially did not provide satisfactory results, further optimization of the catalyst system and the reaction conditions was deemed necessary.

To sum up, very good results could be obtained with the substrates **38** to **41** (entries 1 to 4), with enantioselectivities up to 97% ee. Substitution in position 3 and also in position 4 seemed to decrease the reactivity and as a result, it was necessary to increase the catalyst loading from 10 mol% to 20 mol% for the substituted substrates **39** to **41**.

Table 9: Substrate scope.



entry ^[a]	substrate	catalyst salt	ee [%] ^[b]	yield [%]
1 ^[c]		A	97	74 ^[d]
		B	94	72 ^[d]
2 ^[e]		A	87	75 ^[d]
		B	86	73 ^[d]
3 ^[f]		A	88	59 ^[d]
		B	89	56 ^[d]
4 ^[e]		A	87	71 ^[d]
		B	86	75 ^[d]
5		A	-	-
		B	-	-
6 ^[g]		A	-	-
		B	n.d.	40 ^[h]
7 ^[i]		A	-	-
		B	84	32 ^[h]

^[a] Reaction carried out using 0.25 mmol ketone and 0.21 mmol reactant.

^[b] Determined via chiral HPLC on an AS-H column (*n*-hexane/*i*-propanol 90:10, 1 ml/min).

^[c] Using 10 mol% catalyst and 24 h reaction time.

^[d] Isolated yield obtained after column chromatography.

^[e] Using 20 mol% catalyst and 48 h reaction time.

^[f] Using 20 mol% catalyst and 73 h reaction time.

^[g] Using 20 mol% catalyst and 96 h reaction time.

^[h] Conversion determined via NMR.

^[i] Using 20 mol% catalyst and 120 h reaction time.

4.6 Mechanism

The mechanism of this asymmetric catalytic aziridination is proposed to proceed via an iminium-enamine tandem reaction³⁴, which was already described in section 1.2.3. In Figure 46, the catalytic cycle as well as the corresponding catalyst system of the reaction is shown. The diamine component is represented in orange and the phosphoric acid is drawn in blue. For simplification of the representation of the mechanism, the phosphoric acid counteranion is abbreviated with A^- within the catalytic cycle.

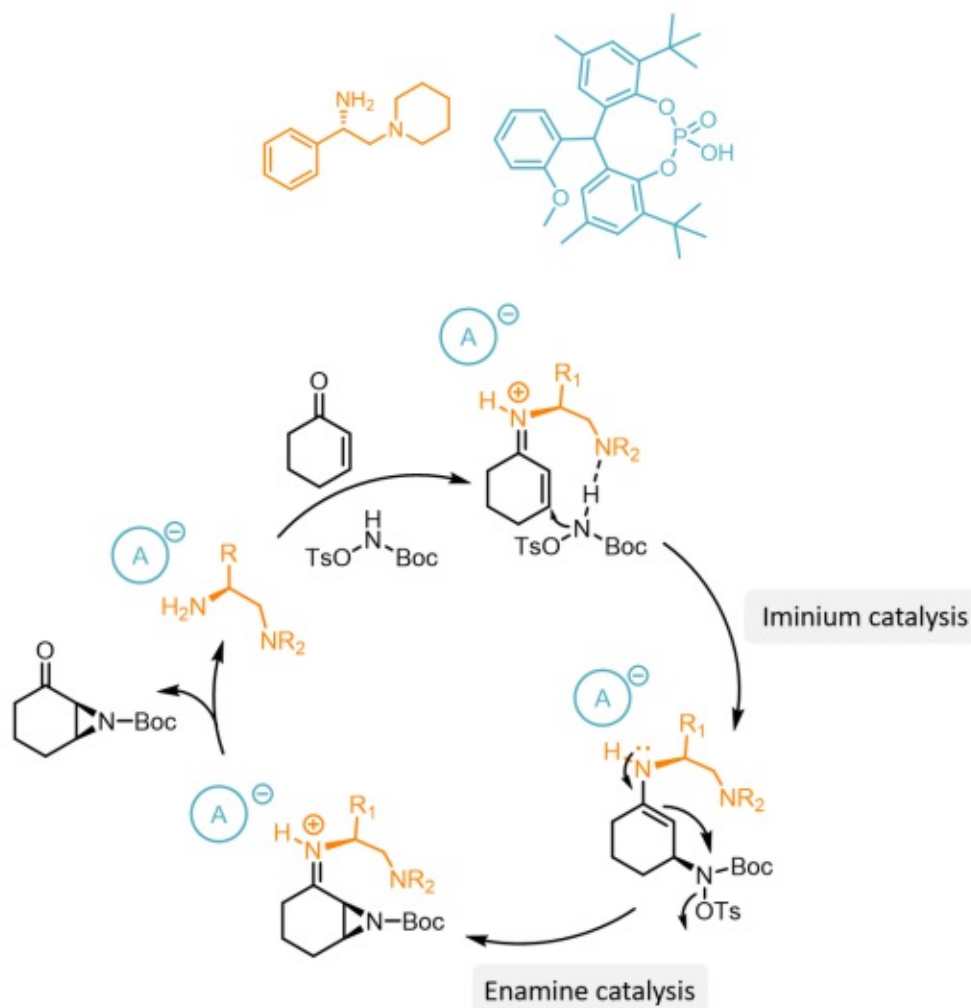


Figure 46: Proposed mechanism for the asymmetric aziridination.

In a first step, the diamine condenses with the carbonyl group of the substrate and a cationic iminium intermediate is formed. Via hydrogen-bonding interactions between the tertiary amine of the catalyst and the hydrogen of the reactant, the N-containing reactant gets directed and can add to the double bond as a nucleophile in an iminium catalysis fashion. The reactant now

becomes electrophilic and the three-membered aziridine heterocycle is formed via an enamine catalysis. The leaving group of the reactant gets cleaved and the cationic iminium intermediate is reformed. Cleavage of the desired product, gives the recovered catalyst, which can be used for further catalytic cycles. Throughout the reaction, the enantioselectivity is not only influenced by the diamine and the direction of the reactant, but the phosphoric acid counteranion has a significant impact on the enantioselectivity as well.

5 Conclusion

In the present work, the concept of counterion enhanced organocatalysis was successfully applied to the asymmetric aziridination of cyclic enones (Figure 47). Therefore, different amines and phosphoric acids were screened, to determine the best performing catalyst system. The optimized catalyst, affording the best enantioselectivity and reactivity, is shown in Figure 47, with both enantiomers of the diamine marked in orange and the phosphoric acid component marked in blue. Considering the synthesis of the catalyst components, cheap and straightforward synthetic routes could be developed. In order to find the optimal reaction conditions, different bases, base equivalents and solvents were screened, which proved to be 2 equivalents of NaHCO_3 and chloroform as the solvent. Furthermore, different reactants were tested, showing that the tosylated Boc-protected hydroxylamine is necessary to achieve good selectivities.

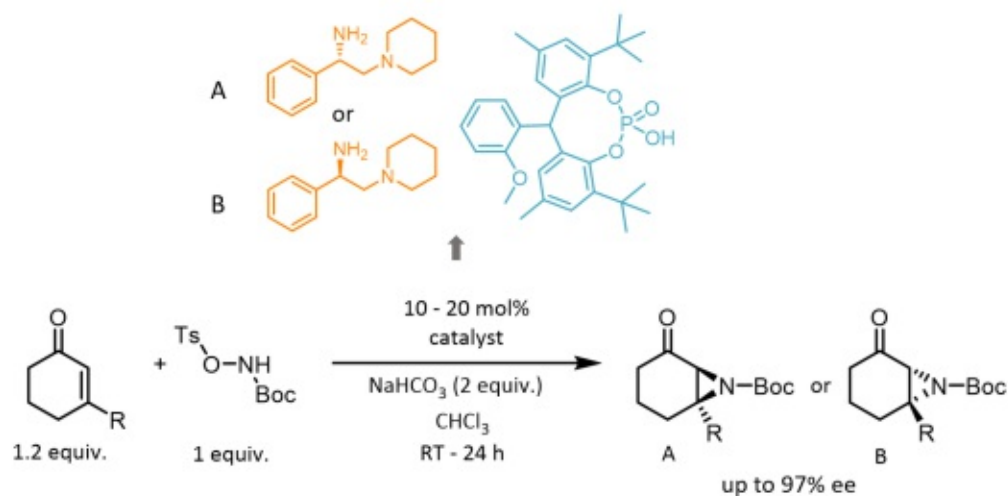


Figure 47: Asymmetric aziridination of cyclic enones via counterion enhanced organocatalysis with the optimized catalyst system.

With all the optimized parameters, a set of 3- and 4- substituted cyclohexenones were used to determine the substrate scope and limitations. Depending on the reactivity of the substrate, a catalyst loading between 10 and 20 mol% had to be used. With all the substrates, excellent enantioselectivities of up to 97% ee and good yields could be observed, thus, demonstrating the versatility of this organocatalytic method for the asymmetric aziridination of cyclic enones.

6 Experimental Part

6.1 Materials and Methods

All chemicals were purchased from commercial suppliers and were used without further purification. Dry solvents were pre-distilled and desiccated on Al_2O_3 columns (PURESOLV, Innovative Technology). Column chromatography was performed on manual glass columns using pre-distilled solvents and silica gel from Merck (40-60 μm). TLC-analyses were done with precoated aluminium-backed plates which were purchased from Merck (silica gel 60 F₂₅₄). UV active compounds were detected at 254 nm, non-UV active compounds were detected using vanillin as staining agent (5% H_2SO_4 and vanillin in EtOH).

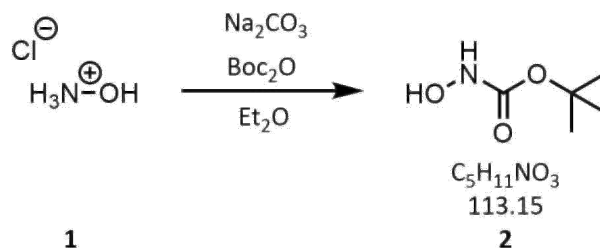
^1H - and ^{13}C - NMR spectra were recorded from CDCl_3 on a Bruker Advanced UltraShield 200 MHz or 400 MHz spectrometer. Chemical shifts are reported in ppm, using tetramethylsilane (TMS) as internal standard and coupling constants (J) are reported in Hz. The following abbreviations were used to explain the NMR spectra: s = singlet, d = doublet, dd = doublet of doublets, ddd = doublet of doublet of doublets, td = triplet of doublets, m = multiplet, brs = broad singlet.

Conversions were determined via ^1H - NMR or GC by using a BGB5 column in combination with a mass spectrometric detection. Enantiomeric excess was determined via HPLC on a DIONEX UPLC, with a PDA plus detector (190-360 nm), using an AS-H (250 \times 4.60 mm, 5 μm) column as the stationary phase and *n*-hexane/*i*-propanol 90:10 as the mobile phase with a flow rate of 1 ml/min. Optical rotation, to determine the absolute configuration, was measured on an Anton Paar MCP500 polarimeter at the specific conditions and the results have been compared to literature values. Concentrations are given in g/100 ml.

HR-MS analysis was carried out using HTC PAL system auto sampler, an Agilent 1100/1200 HPLC and Agilent 6230 AJS ESI-TOF mass spectrometer. Melting point measurements were carried out using a BÜCHI Melting Point B-540. Infrared spectra were recorded on a Perkin-Elmer Spectrum 65 FT IR spectrometer equipped with a specac MK II Golden Gate Single Reflection ATR unit.

6.2 Reactant synthesis

6.2.1 *tert*-Butyl hydroxycarbamate (2)

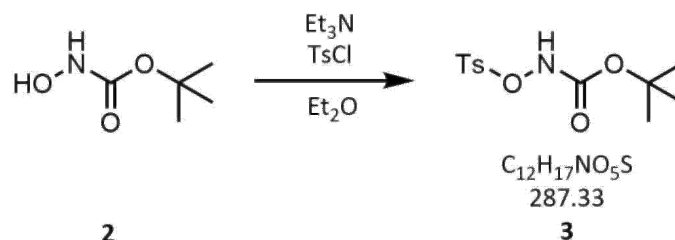


Compound **2** was prepared according to the following modified literature procedure.⁴⁰

A suspension of hydroxylamine hydrochloride (**1**, 10 g, 144 mmol, 1.0 equiv.) and Na_2CO_3 (7.6 g, 72 mmol, 0.5 equiv.) in Et_2O (62 ml) and H_2O (2 ml) was stirred for approx. 1 h at room temperature with evolution of CO_2 . A solution of *tert*-butyl dicarbonate (21 g, 96 mmol) in Et_2O (41 ml) was then added dropwise at 0 °C and the suspension was stirred at room temperature over night. The organic phase was decanted, the solids were washed with Et_2O . The combined organic solutions were evaporated to dryness and dried in vacuum. Product **2** was obtained as a colourless solid (12 g, 63%).

$^1\text{H-NMR}$ (400 MHz, CDCl_3) δ 7.04 (brs, 2H), 147 (s, 9H).

Analytical data was in accordance with the literature.⁴⁰

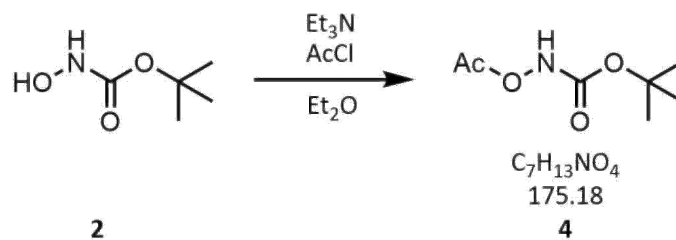
6.2.2 *tert*-Butyl (tosyloxy)carbamate (**3**)

Compound **3** was prepared according to the following literature procedure.⁴¹

To a solution of *tert*-butyl hydroxycarbamate (**2**, 11.8 g, 89 mmol, 1.0 equiv.) and TsCl (17.7 g, 93 mmol, 1.1 equiv.) in Et₂O (350 ml) at 0 °C was added Et₃N (12.9 ml, 93 mmol, 1.1 equiv.) dropwise. The mixture was stirred at 0 °C for 20 minutes, and then was warmed to room temperature and stirred for 4 hours. The reaction mixture was filtered, and the solid was rinsed with Et₂O. The filtrate was concentrated in vacuo to afford the crude product, which was suspended in hexane (150 ml) and stirred at room temperature for 30 minutes. The mixture was filtered, and the resulting solid was rinsed with hexane and subsequently dried in vacuo to afford product **3** as a colourless solid (24.2 g, 95%).

¹H-NMR (400 MHz, CDCl₃) δ 7.88 (d, *J* = 8.4 Hz, 2H), 7.73 (s, 1H), 7.36 (d, *J* = 8.0 Hz, 2H), 2.45 (s, 3H), 1.29 (s, 9H).

Analytical data was in accordance with the literature.⁴¹

6.2.3 *tert*-Butyl acetoxy carbamate (4)

Compound **4** was prepared according to the following modified literature procedure.⁴²

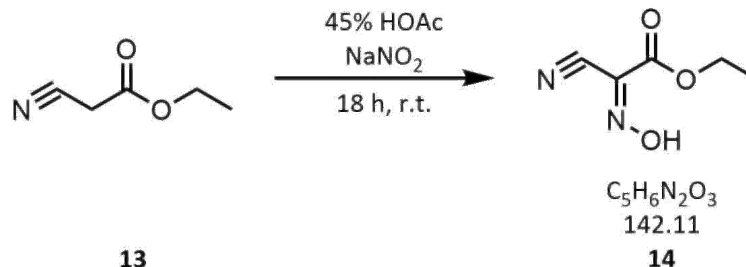
To a solution of *tert*-butyl hydroxycarbamate (**2**, 1.0 g, 7.5 mmol, 1.0 equiv.) dissolved in Et₂O (30 ml), Et₃N (1.1 ml, 7.9 mmol, 1.1 equiv.) was added at 0 °C. Then acetyl chloride (0.6 ml, 7.9 mmol, 1.1 equiv.) was added dropwise. The reaction mixture was stirred for 30 min at 0 °C and then 30 min at room temperature. The white solid formed in the reaction was filtered off. The filtrate was washed with saturated aqueous NaHCO₃ solution and water, dried over Na₂SO₄, and filtered. The filtrate was concentrated under reduced pressure to afford the product **4** as a colourless liquid (1.0 g, 77%).

¹H-NMR (400 MHz, CDCl₃) δ 7.93 (s, 1H), 2.19 (s, 3H), 1.48 (s, 9H).

Analytical data was in accordance with the literature.⁴²

6.3 Diamine synthesis

6.3.1 1-Cyano-2-ethoxy-2-oxoethaniminium 4-methylbenzenesulfonate (**14**)

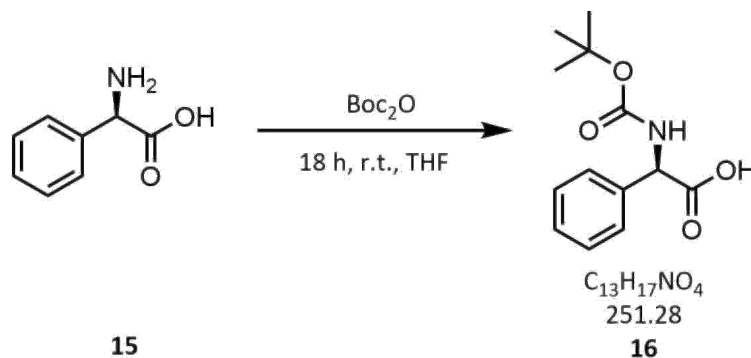


Compound **14** was prepared according to the following literature procedure.⁴³

A solution of ethyl cyanoacetate (**13**, 10 g, 88 mmol, 1.0 equiv.) in aqueous acetic acid (45%, 40 ml) was stirred at 0 °C for 15 min. Sodium nitrite (18.3 g, 265 mmol, 3.0 equiv.) was added portion-wise and the reaction mixture was stirred for 18 h at room temperature. Et₂O (50 ml) and water were added, until a clear solution was observed. The aqueous phase was extracted with Et₂O (2x) and the combined organic phase was washed with water (2x) and brine (1x). Removal of the solvent gave the product **14** as a yellow solid (12.2 g, 98%).

¹H-NMR (400 MHz, CDCl₃) δ 4.45 (q, *J* = 7.1 Hz, 2H), 1.41 (t, *J* = 7.1 Hz, 3H).

Analytical data was in accordance with the literature.⁴³

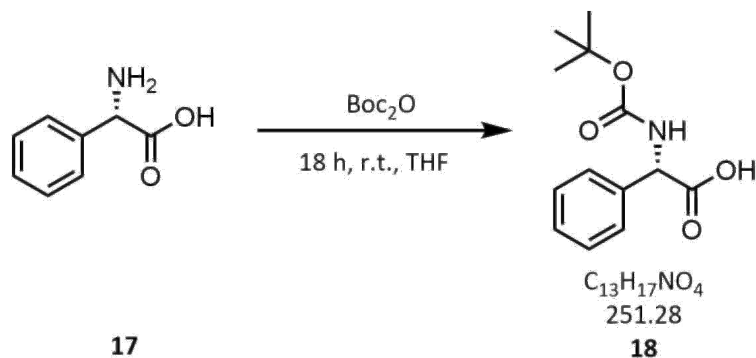
6.3.2 (*R*)-2-((*tert*-Butoxycarbonyl)amino)-2-phenylacetic acid (**16**)

Compound **16** was prepared according to the following modified literature procedure.³⁵

To a solution of D-phenylglycine (**15**, 3 g, 20 mmol, 1.0 equiv.) in a mixture of THF (23 ml) and 1 N NaOH (24 ml or more until clear solution), di-*tert*-butylcarbonate (5.5 ml, 24 mmol, 1.2 equiv.) was added at room temperature. The solution was stirred for 18 h at room temperature. Then THF was removed in vacuum, the resulting aqueous solution was diluted with DCM (25 ml) and acidified to pH 2 with a 2 N HCl solution. The aqueous phase was extracted with DCM (3x), the resulting organic phase was extracted with brine and dried over anhydrous Na₂SO₄. Removal of the solvent gave the product **16** as a viscous oil (4.7 g, 94%).

¹H-NMR (400 MHz, CDCl₃) δ 7.51 (brs, 1H), 7.29 - 7.43 (m, 5H), 5.13 (d, *J* = 8.1 Hz, 1H), 1.40 (s, 9H).

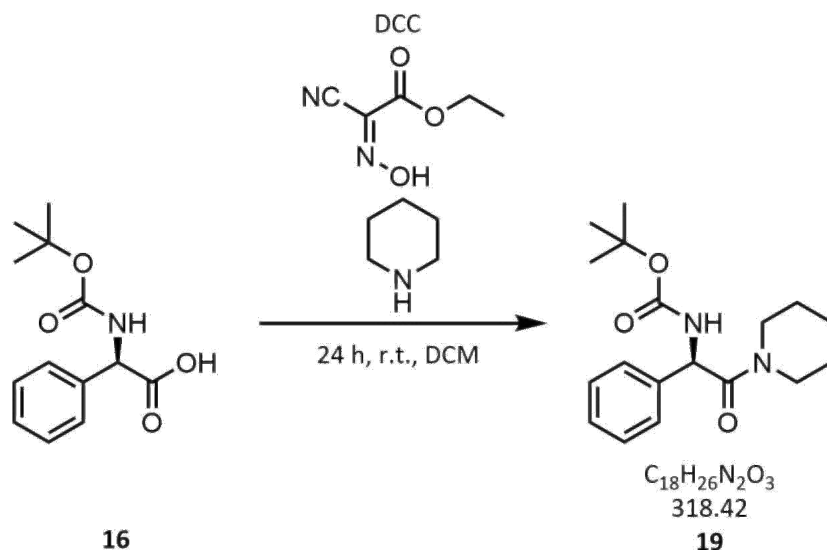
Analytical data was in accordance with the literature.³⁵

6.3.3 (*S*)-2-((*tert*-Butoxycarbonyl)amino)-2-phenylacetic acid (**18**)

Prepared according to procedure 6.3.2 from L-phenylglycine (**17**, 3 g, 20 mmol, 1.0 equiv.) in a mixture of THF (23 ml) and 1 N NaOH (24 ml) and di-*tert*-butylcarbonate (5.5 ml, 24 mmol, 1.2 equiv.) to give the product **18** as a viscous oil (4.9 g, 98%).

¹H-NMR (400 MHz, CDCl₃) δ 7.51 (brs, 1H), 7.29 - 7.43 (m, 5H), 5.13 (d, $J = 8.1$ Hz, 1H), 1.40 (s, 9H).

Analytical data was in accordance with the literature.³⁵

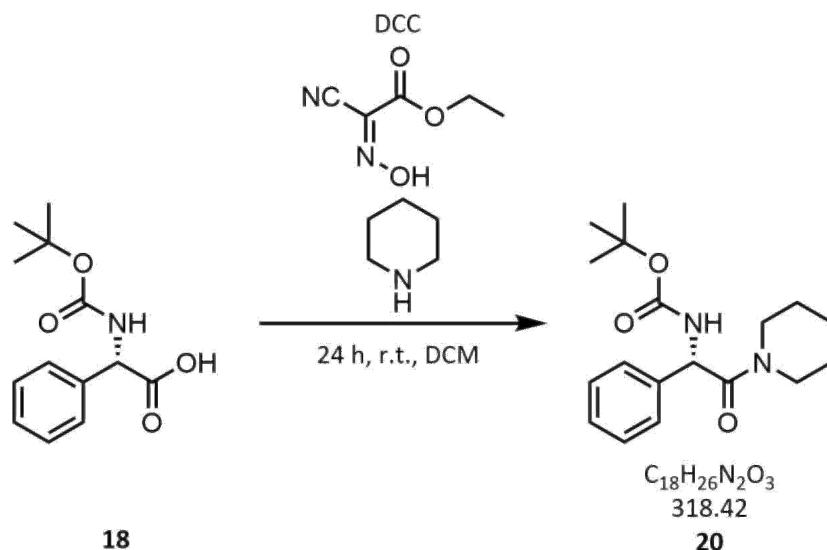
6.3.4 *tert*-Butyl-(*R*)-(2-oxo-1-phenyl-2-(piperidin-1-yl)ethyl)carbamate (**19**)

Compound **19** was prepared according to the following modified literature procedure.³⁶

To a solution of (*R*)-2-((*tert*-butoxycarbonyl)amino)-2-phenylacetic acid (**16**, 5.6 g, 22.3 mmol, 1 equiv.) in dry DCM, DCC (9 g, 43.6 mmol, 2equiv.), oxyma (3.5 g, 24.6 mmol, 1.1 equiv.) and piperidine (4.7 ml, 47.6 mmol, 2.1 equiv.) were added at 0 °C. The resulting turbid solution was stirred another 15 min at 0 °C, allowed to warm up and stirred at room temperature for 24 h. Then cold EtOAc (200 ml) was added, the mixture was stirred for 5 min, DCU was filtered off and the clear solution was concentrated in vacuum. To the crude mixture EtOAc (100 ml) was added and extracted with 1 N HCl (1x). The formed solid was filtered off and the filtrate repeatedly extracted with 1 N HCl (1x) followed by extraction with 1 N NaOH (2x) and brine (1x). The organic phase was dried over anhydrous Na₂SO₄ and concentrated in vacuo. Purification via column chromatography (30% EtOAc/PE) yielded the product **19** as a colourless solid (5.9 g, 83%).

¹H-NMR (400 MHz, CDCl₃) δ 7.41 - 7.24 (m, 5H), 6.12 (d, *J* = 7.6 Hz, 1H), 5.55 (d, *J* = 7.7, 1H), 3.78 - 3.67 (m, 1H), 3.47 - 3.37 (m, 1H), 3.34 - 3.21 (m, 2H), 1.59 - 1.47 (m, 3H), 1.40 (s, 12H).

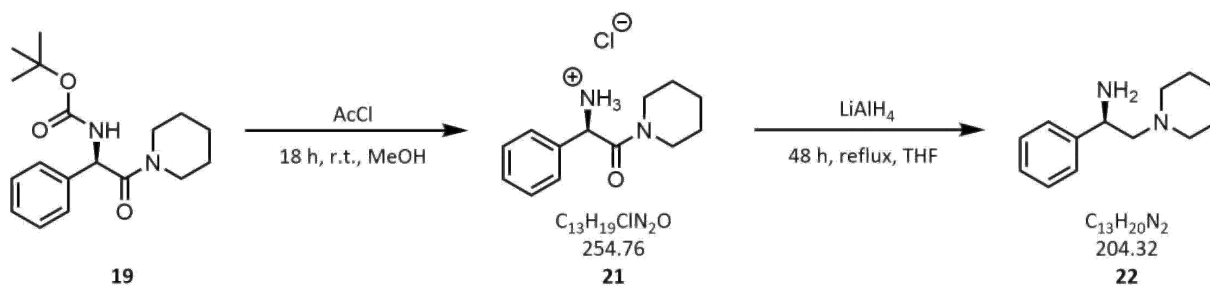
Analytical data was in accordance with the literature.³⁶

6.3.5 *tert*-Butyl-(*S*)-(2-oxo-1-phenyl-2-(piperidin-1-yl)ethyl)carbamate (**20**)

Prepared according to procedure 6.3.4 from (*S*)-2-((*tert*-butoxycarbonyl)amino)-2-phenylacetic acid (**18**, 4.9 g, 19.5 mmol, 1.0 equiv.) in dry DCM, DCC (7.9 g, 38.3 mmol, 2.0 equiv.), oxyma (2.9 g, 20.4 mmol, 1.1 equiv.) and piperidine (4.2 ml, 42.5 mmol, 2.2 equiv.) Purification via column chromatography (30% EtOAc/PE) gave the product **20** as a colourless solid (5.5 g, 86%).

$^1\text{H-NMR}$ (400 MHz, CDCl_3) δ 7.41 - 7.24 (m, 5H), 6.12 (d, $J = 7.6$ Hz, 1H), 5.55 (d, $J = 7.7$, 1H), 3.78 - 3.67 (m, 1H), 3.47 - 3.37 (m, 1H), 3.34 - 3.21 (m, 2H), 1.59 - 1.47 (m, 3H), 1.40 (s, 12H).

Analytical data was in accordance with the literature.³⁶

6.3.6 (*R*)-1-Phenyl-2-(piperidin-1-yl)ethan-1-amine (**22**)

Compound **21** was prepared according to the following modified literature procedure.³⁶

To a solution of *tert*-butyl-(*R*)-(2-oxo-1-phenyl-2-(piperidin-1-yl)ethyl)carbamate (**19**, 5.9 g, 18.5 mmol, 1.0 equiv.), in dry MeOH (48 ml), acetyl chloride (10.6 ml, 148.6 mmol, 8.0 equiv.) was added at 0 °C. After 15 min the ice bath was removed and the solution was stirred for another 18 h. The solvent was then evaporated and the solid dried in vacuum. Et₂O was then added to the solid and the dispersion was stirred for 15 min, the product was filtered, dried in vacuum and used directly for the next step without further purification. The intermediate **21** could be obtained as a light green solid (4.3 g, 92%).

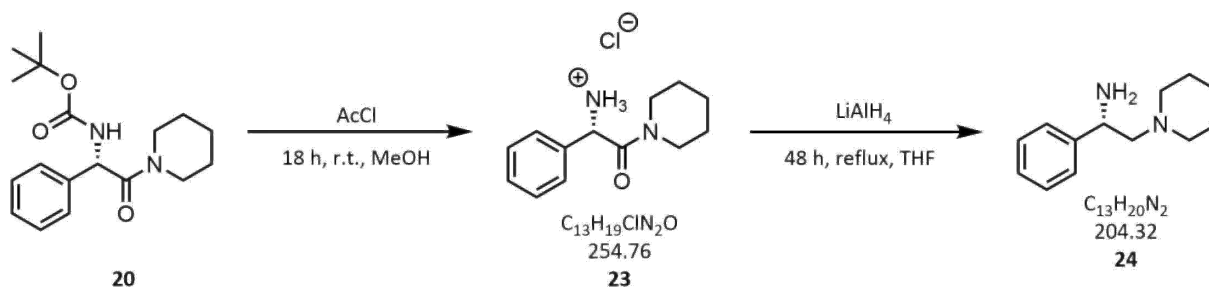
Compound **22** was prepared according to the following modified literature procedure.³⁷

To a stirred solution of (*R*)-2-oxo-1-phenyl-2-(piperidin-1-yl)ethan-1-aminium chloride (**21**, 4.8 g, 18.7 mmol, 1.0 equiv.) in dry THF (140 ml), LiAlH₄ (3 g, 79.1 mmol, 4.2 equiv.) was added in portions at 0 °C. The resulting dispersion was stirred for another 15 min at room temperature and heated to 80 °C for 48 h. After cooling to room temperature, dest. H₂O (1 ml per g LiAlH₄), and 15% aqueous NaOH (2 ml per g LiAlH₄) were added at 0 °C and the mixture was stirred for 10 min. Then anhydrous Na₂SO₄ was added to remove the previously added water followed by EtOAc (70 ml). The solid was filtered off and washed with EtOAc. The organic phase was then extracted with 1 N NaOH (2x) and brine (1x). The solvent was evaporated and purification via column chromatography (10% MeOH in DCM + 0.8% Et₃N) gave the diamine **22** as a yellow oil (2.1 g, 55%).

¹H-NMR (400 MHz, CDCl₃) δ 7.41 – 7.27 (m, 5H), 4.13 (dd, *J* = 10.4, 3.6 Hz, 1H),
 2.68 – 2.55 (m, 2H), 2.47 – 2.30 (m, 4H), 2.16 (s, 2H),
 1.69 – 1.51 (m, 4H), 1.49 – 1.37 (m, 2H).

Analytical data was in accordance with the literature.³⁷

6.3.7 (S)-1-Phenyl-2-(piperidin-1-yl)ethan-1-amine (24)



Compound **23** was prepared according to procedure 6.3.6 from *tert*-butyl-(S)-(2-oxo-1-phenyl-2-(piperidin-1-yl)ethyl)carbamate (**20**, 5.5 g, 17.3 mmol, 1 equiv.) in dry MeOH (44 ml), acetyl chloride (9.9 ml, 138.7 mmol, 8.0 equiv.) to give the intermediate **23** as a light green solid (4.1 g, 93%) which was used for the next step without further purification.

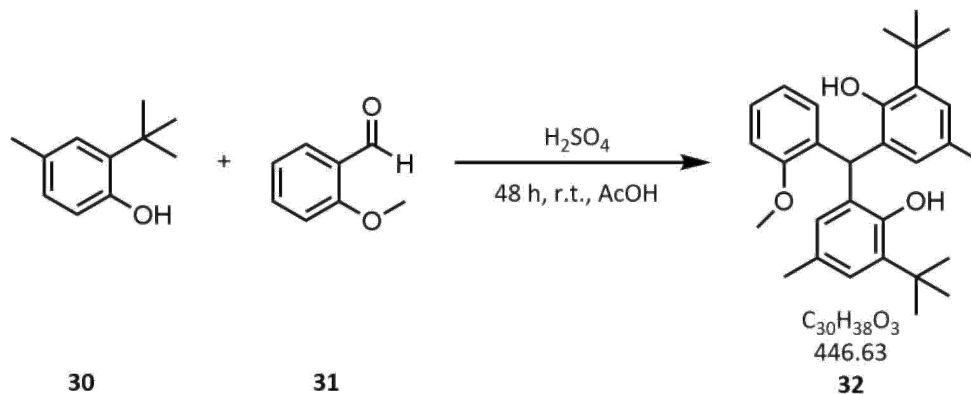
Compound **24** was prepared according to procedure 6.3.6 from (S)-2-oxo-1-phenyl-2-(piperidin-1-yl)ethan-1-aminium chloride (**23**, 3.8 g, 18.8 mmol, 1 equiv.) in dry THF (110 ml), LiAlH₄ (2.4 g, 63.2 mmol, 3.4 equiv.) to give the diamine **24** as a yellow oil (2.4 g, 78%).

¹H-NMR (400 MHz, CDCl₃) δ 7.35 – 7.15 (m, 6H), 4.06 (dd, *J* = 10.3, 3.7 Hz, 1H),
2.62 – 2.47 (m, 2H), 2.39 – 2.21 (m, 4H), 1.83 (s, 2H),
1.62 – 1.44 (m, 4H), 1.42 - 1.32 (m, 2H).

Analytical data was in accordance with the literature.³⁷

6.4 Phosphoric acid synthesis

6.4.1 6,6'-((2-Methoxyphenyl)methylene)bis(2-(*tert*-butyl)-4-methylphenol) (**32**)

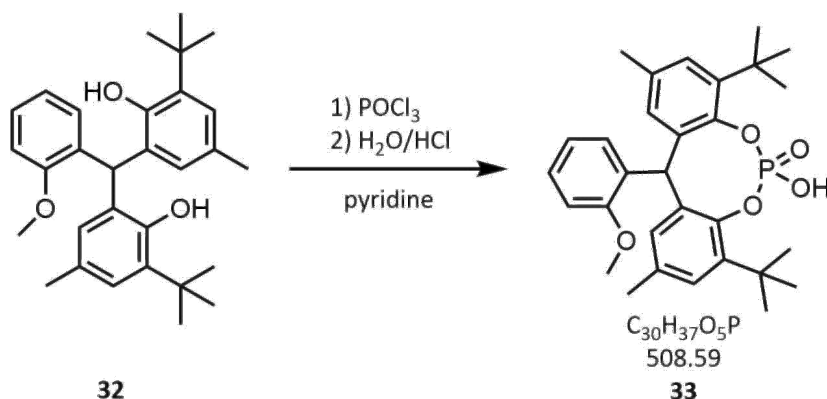


Compound **32** was prepared according to the following modified literature procedure.³⁸

To a solution of 2-(*tert*-butyl)-4-methylphenol (**30**, 1 g, 6 mmol, 1.0 equiv.) in acetic acid (0.58 M) was added 2-methoxybenzaldehyde (**31**, 0.5 equiv.) at room temperature. Concentrated sulfuric acid (1.3 equiv.) was added dropwise at about 10 °C and stirred for 15 min. The ice / water bath was removed and the yellow coloured solution was stirred for 18 h at room temperature. Dest. H₂O was added, the precipitate filtered and subsequently washed with dest. H₂O until the filtrate was colourless. The crude precipitate was dissolved in DCM, extracted with sat. NaHCO₃ (2x), brine (1x), the combined organic phase dried over anhydrous Na₂SO₄ and concentrated. Purification via column chromatography (3 % EtOAc in PE) gave the product **32** as a red solid (1.6 g, 59%).

¹H-NMR (200 MHz, CDCl₃) δ 7.37 – 7.21 (m, 1H), 7.09 – 6.86 (m, 5H), 6.55 (d, *J* = 2.1 Hz, 2H), 5.91 (s, 1H), 4.95 (s, 2H), 3.81 (s, 3H), 2.19 (s, 6H), 1.37 (s, 18H).

6.4.2 4,8-Di-*tert*-butyl-6-hydroxy-12-(2-methoxyphenyl)-2,10-dimethyl-12*H*-dibenzo-*[d,g]*[1,3,2]dioxaphosphocine 6-oxide (**33**)



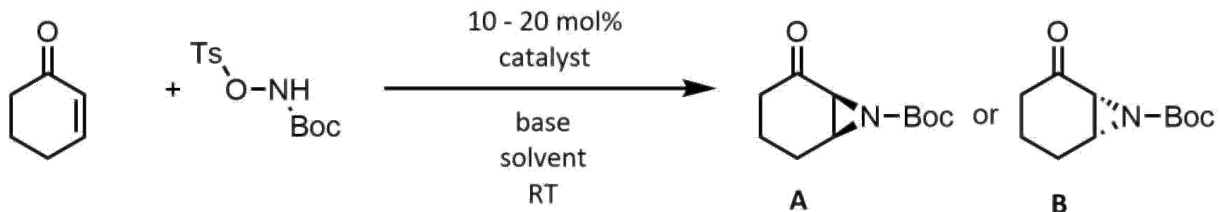
Compound **33** was prepared according to the following modified literature procedure.³⁹

To a solution of 6,6'-((2-methoxyphenyl)methylene)bis(2-(*tert*-butyl)-4-methylphenol) (**32**, 1.6 g, 3.6 mmol, 1.0 equiv.) in pyridine (0.34 M), phosphoroylchloride (2.0 equiv.) was added slowly via syringe at 0 °C. After stirring the reaction mixture for 24 h at 95 °C, it was cooled to room temperature and H₂O (25 equiv.) was added slowly. The resulting clear solution was stirred for another 18 h at 95 °C. After cooling to room temperature, 4 N HCl was added slowly. The precipitate was filtered and washed with 4 N HCl. Dichloromethane was added and the organic phase was washed several times with 4 N HCl (3 × 25 ml) followed by brine and H₂O and dried over anhydrous Na₂SO₄. Removal of the solvent gave the product **33** as a colourless solid (1.6 g, 88%).

Melting Point	167 - 169 °C
¹H-NMR (400 MHz, CD ₂ Cl ₂)	δ 10.08 (s, 2H), 7.64 (ddd, <i>J</i> = 7.8, 1.6, 0.8 Hz, 1H), 7.27 (td, <i>J</i> = 7.7, 1.6 Hz, 1H), 7.05 (s, 2H), 7.02 – 6.93 (m, 3H), 6.87 (dd, <i>J</i> = 8.2, 1.2 Hz, 1H), 6.47 (s, 1H), 3.52 (s, 3H), 2.25 (s, 6H), 1.42 (s, 18H).
¹³C-NMR (101 MHz, CD ₂ Cl ₂)	δ 158.54, 147.36, 147.27, 141.03, 140.97, 134.70, 134.67, 134.30, 134.29, 129.75, 129.34, 128.36, 127.88, 127.86, 126.99, 120.27, 112.13, 56.08, 38.08, 35.25, 31.15, 21.33.
³¹P-NMR (162 MHz, CD ₂ Cl ₂)	δ -10.56.
HRMS (ESI-TOF)	<i>m/z</i> calcd for C ₃₀ H ₃₇ O ₅ P: 507.2306; found: 507.2304.
IR ATR (ν _{max} /cm ⁻¹)	2960 (O-H), 1599 (C=C), 1436 (C-O), 1199 (C-H), 955 (C-H arom.).

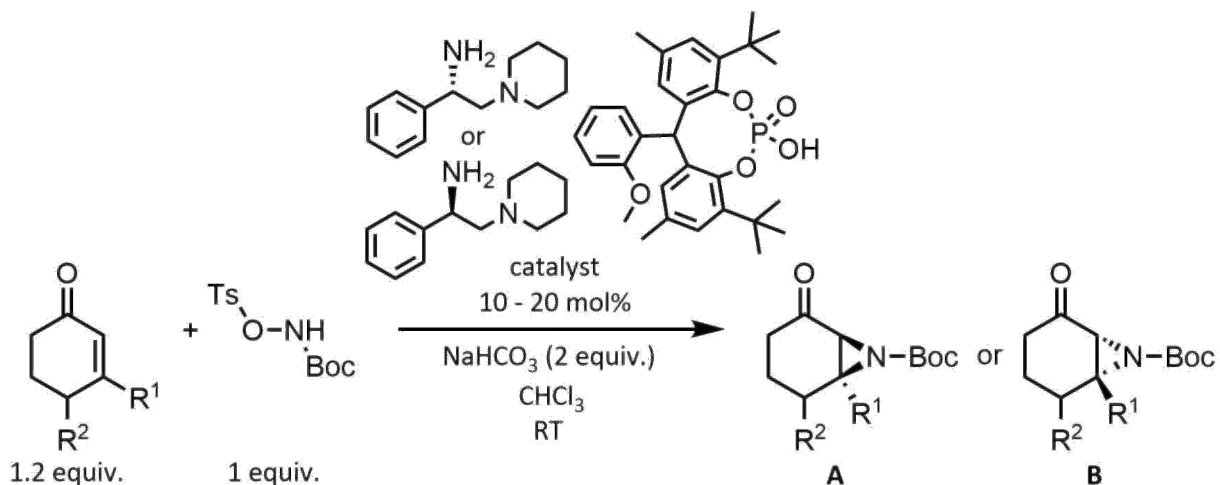
6.5 Asymmetric aziridination of cyclic enones

6.5.1 General procedure for parameter optimization



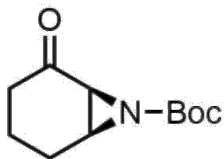
In a 8 ml screw-cap vial equipped with a Teflon-coated stirring bar, the catalyst (0.02 - 0.04 mmol, 10 - 20 mol%), consisting of a phosphoric acid (1.0 equiv.) and an amine (1.0 equiv.), was dissolved in an appropriate solvent (0.25 M) and the formed catalyst salt was stirred for 30 min at room temperature. Then cyclic enone was added (0.25 mmol, 1.2 equiv.) and the solution stirred for another 10 min. *Tert*-butyl (tosyloxy)carbamate (**3**, 0.21 mmol, 1.0 equiv.) was added and after 5 min of stirring base (0.42 mmol, 2.0 equiv.) was added. The reaction mixture was then stirred at room temperature for 24 - 48 h. The crude reaction mixture was filtered and the filtrate concentrated under reduced pressure. Light petroleum was added to the residue and the catalyst filtered off. The solvent was removed under reduced pressure. Conversions and yields were determined via $^1\text{H-NMR}$ spectroscopy and the enantiomeric excess was determined via chiral HPLC measurements.

6.5.2 General procedure for scope and limitations



In a 20 ml screw-cap vial equipped with a Teflon-coated stirring bar, the catalyst (0.08 - 0.3 mmol, 5 - 20 mol%), consisting of the phosphoric acid (**33**, 1.0 equiv.) and L-phenylglycine-piperidine (**24**) or D-phenylglycine-piperidine (**22**, 1.0 equiv.), was dissolved in CHCl_3 (0.25 M) and the formed catalyst salt was stirred for 30 min at room temperature. Then a cyclic enone was added (1.87 mmol, 1.2 equiv.) and the solution stirred for another 10 min. *Tert*-butyl (tosyloxy)carbamate (**3**, 1.56 mmol, 1.0 equiv.) was added and after 5 min of stirring NaHCO_3 (3.12 mmol, 2.0 equiv.) was added. The reaction mixture was then stirred at room temperature for 24 - 96 h. The crude reaction mixture was extracted with brine (1x) and the aqueous phase extracted with EtOAc (3x). The organic phase was dried over Na_2SO_4 and the solvent was removed under reduced pressure. Purification via column chromatography (20% EtOAc in PE, vanillin staining agent) gave the desired products.

6.5.3 Analytical data of the aziridines

***tert*-Butyl (1*S*,6*S*)-2-oxo-7-azabicyclo[4.1.0]heptane-7-carboxylate**

¹H-NMR (400 MHz, CDCl₃) δ 3.08 - 3.05 (m, 1H), 2.88 (d, *J* = 5.8 Hz, 1H), 2.53 - 2.40 (m, 1H), 2.27 - 2.19 (m, 1H), 2.09 - 1.90 (m, 2H), 1.82 - 1.73 (m, 1H), 1.67 - 1.59 (m, 1H), 1.44 (s, 9H).

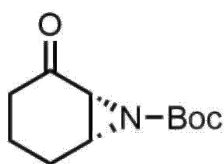
¹³C-NMR (101 MHz, CDCl₃) δ 204.3, 160.6, 82.2, 43.2, 40.4, 36.9, 27.8, 22.6, 17.3.

Enantiomeric excess 97%
Determined via chiral HPLC on an AS-H column (*n*-hexane/*i*-propanol 90:10, 1 ml/min).

α_D²⁰ - 143.5 (c = 1.0, CHCl₃)

Yield (isolated) 74%

Analytical data was in accordance with the literature.³⁴

***tert*-Butyl (1*R*,6*R*)-2-oxo-7-azabicyclo[4.1.0]heptane-7-carboxylate**

¹H-NMR (400 MHz, CDCl₃) δ 3.09 - 3.05 (m, 1H), 2.88 (d, *J* = 5.9 Hz, 1H), 2.53 - 2.44 (m, 1H), 2.27 - 2.19 (m, 1H), 2.09 - 1.90 (m, 2H), 1.82 - 1.73 (m, 1H), 1.69 - 1.59 (m, 1H), 1.44 (s, 9H).

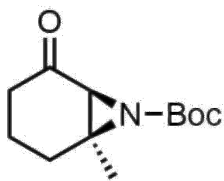
¹³C-NMR (101 MHz, CDCl₃) δ 204.4, 160.7, 82.4, 43.3, 40.5, 37.0, 28.0, 22.7, 17.4.

Enantiomeric excess 94%
Determined via chiral HPLC on an AS-H column (*n*-hexane/*i*-propanol 90:10, 1 ml/min).

α_D²⁰ + 107.6 (c = 1.0, CHCl₃)

Yield (isolated) 72%

Analytical data was in accordance with the literature.³⁴

***tert*-Butyl (1*S*,6*S*)-1-methyl-5-oxo-7-azabicyclo[4.1.0]heptane-7-carboxylate**

¹H-NMR (400 MHz, CDCl₃) δ 2.77 (s, 1H), 2.50 - 2.37 (m, 1H), 2.16 - 2.09 (m, 1H), 2.06 - 1.92 (m, 2H), 1.71 - 1.57 (m, 2H), 1.45 (s, 9H), 1.39 (s, 3H).

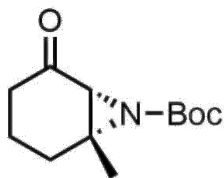
¹³C-NMR (101 MHz, CDCl₃) δ 205.6, 159.0, 82.0, 49.68, 47.6, 36.2, 29.3, 28.1, 20.4, 17.5.

Enantiomeric excess 87%
Determined via chiral HPLC on an AS-H column (*n*-hexane/*i*-propanol 90:10, 1 ml/min).

α_D²⁰ - 80.7 (c = 1.0, CHCl₃)

Yield (isolated) 75%

Analytical data was in accordance with the literature.³⁴

***tert*-Butyl (1*R*,6*R*)-1-methyl-5-oxo-7-azabicyclo[4.1.0]heptane-7-carboxylate**

¹H-NMR (400 MHz, CDCl₃) δ 2.77 (s, 1H), 2.49 - 2.38 (m, 1H), 2.16 - 2.09 (m, 1H), 2.06 - 1.93 (m, 2H), 1.69 - 1.59 (m, 2H), 1.46 (s, 9H), 1.39 (s, 3H).

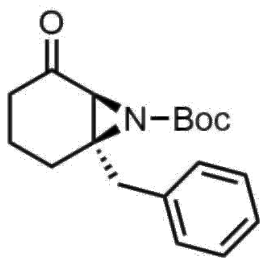
¹³C-NMR (101 MHz, CDCl₃) δ 205.6, 159.0, 82.0, 49.7, 47.6, 36.2, 29.3, 28.1, 20.4, 17.5.

Enantiomeric excess 86%
Determined via chiral HPLC on an AS-H column (*n*-hexane/*i*-propanol 90:10, 1 ml/min).

α_D²⁰ + 81.7 (c = 1.0, CHCl₃)

Yield (isolated) 73%

Analytical data was in accordance with the literature.³⁴

***tert*-Butyl (1*R*,6*S*)-1-benzyl-5-oxo-7-azabicyclo[4.1.0]heptane-7-carboxylate**

¹H-NMR (400 MHz, CDCl₃) δ 7.34 - 7.28 (m, 2H), 7.28 - 7.23 (m, 2H), 7.23 - 7.19 (m, 2H), 3.24 (d, *J* = 14.3 Hz, 1H), 3.06 (s, 1H), 2.47 (d, *J* = 14.2 Hz, 1H), 2.43 - 2.35 (m, 1H), 2.08 - 2.00 (m, 1H), 1.99 - 1.86 (m, 2H), 1.66 - 1.51 (m, 2H), 1.49 (s, 9H).

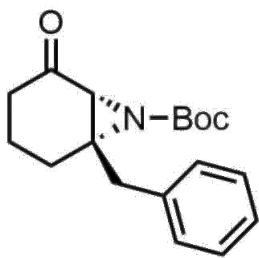
¹³C-NMR (101 MHz, CDCl₃) δ 205.1, 158.6, 136.4, 129.5, 128.9, 127.3, 82.4, 51.3, 48.8, 41.4, 36.2, 28.1, 26.2, 17.6.

Enantiomeric excess 88%
Determined via chiral HPLC on an AS-H column (*n*-hexane/*i*-propanol 90:10, 1 ml/min).

α_D²⁰ - 139.1 (c = 1.0, CHCl₃)

Yield (isolated) 59%

Analytical data was in accordance with the literature.³⁴

***tert*-Butyl (1*S*,6*R*)-1-benzyl-5-oxo-7-azabicyclo[4.1.0]heptane-7-carboxylate**

¹H-NMR (400 MHz, CDCl₃) δ 7.34 - 7.28 (m, 2H), 7.28 - 7.23 (m, 2H), 7.23 - 7.18 (m, 2H), 3.24 (d, *J* = 14.2 Hz, 1H), 3.06 (s, 1H), 2.47 (d, *J* = 14.3 Hz, 1H), 2.43 - 2.35 (m, 1H), 2.08 - 2.00 (m, 1H), 2.00 - 1.86 (m, 2H), 1.61 - 1.52 (m, 2H), 1.49 (s, 9H).

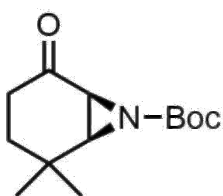
¹³C-NMR (101 MHz, CDCl₃) δ 205.1, 158.6, 136.4, 129.5, 128.9, 127.3, 82.4, 51.3, 48.8, 41.4, 36.2, 28.2, 26.2, 17.6.

Enantiomeric excess 89%
Determined via chiral HPLC on an AS-H column (*n*-hexane/*i*-propanol 90:10, 1 ml/min).

α_D²⁰ + 137.5 (c = 1.0, CHCl₃)

Yield (isolated) 56%

Analytical data was in accordance with the literature.³⁴

***tert*-Butyl (1*S*,6*S*)-2,2-dimethyl-5-oxo-7-azabicyclo[4.1.0]heptane-7-carboxylate**

¹H-NMR (400 MHz, CDCl₃) δ 2.92 (d, *J* = 5.9, 1H), 2.66 (dd, *J* = 5.9, *J* = 1.6 Hz, 1H), 2.35 (ddd, *J* = 19.1, *J* = 6.5, *J* = 2.4 Hz, 1H), 2.21 - 2.11 (m, 1H), 1.96 - 1.84 (m, 1H), 1.44 (s, 9H), 1.32 - 1.24 (m, 1H), 1.21 (s, 3H), 1.03 (s, 3H).

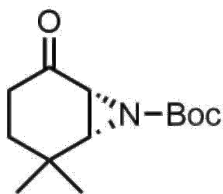
¹³C-NMR (101 MHz, CDCl₃) δ 204.7, 160.5, 82.2, 50.2, 44.2, 33.8, 30.4, 28.0, 27.7, 23.4.

Enantiomeric excess 87%
Determined via chiral HPLC on an AS-H column (*n*-hexane/*i*-propanol 90:10, 1 ml/min).

α_D²⁰ - 100.1 (c = 1.0, CHCl₃)

Yield (isolated) 71%

Analytical data was in accordance with the literature.³⁴

tert-Butyl (1*R*,6*R*)-2,2-dimethyl-5-oxo-7-azabicyclo[4.1.0]heptane-7-carboxylate

¹H-NMR (400 MHz, CDCl ₃)	δ 2.92 (d, <i>J</i> = 5.9, 1H), 2.66 (dd, <i>J</i> = 5.9, <i>J</i> = 1.6 Hz, 1H), 2.35 (ddd, <i>J</i> = 19.1, <i>J</i> = 6.5, <i>J</i> = 2.4 Hz, 1H), 2.22 - 2.10 (m, 1H), 1.97 - 1.84 (m, 1H), 1.44 (s, 9H), 1.32 - 1.24 (m, 1H), 1.21 (s, 3H), 1.03 (s, 3H).
¹³C-NMR (101 MHz, CDCl ₃)	δ 204.7, 160.5, 82.2, 50.2, 44.2, 33.8, 30.4, 27.8, 27.7, 23.4.
Enantiomeric excess	86% Determined via chiral HPLC on an AS-H column (<i>n</i> -hexane/ <i>i</i> -propanol 90:10, 1 ml/min).
α_D²⁰	+ 103.4 (<i>c</i> = 1.0, CHCl ₃)
Yield (isolated)	75%
Analytical data was in accordance with the literature. ³⁴	

7 Appendix

7.1 HPLC-spectra

7.1.1 *tert*-Butyl-2-oxo-7-azabicyclo[4.1.0]heptane-7-carboxylate

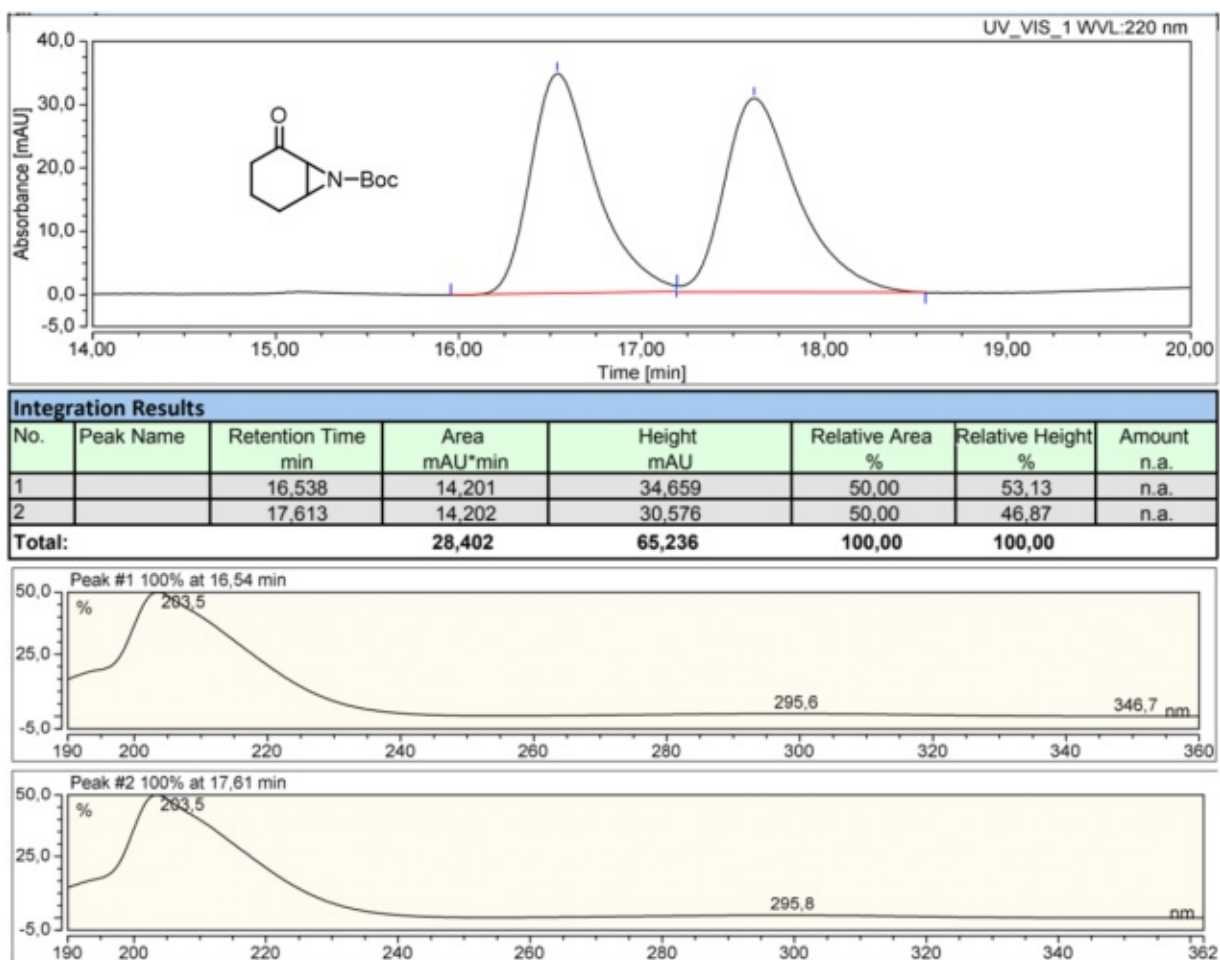
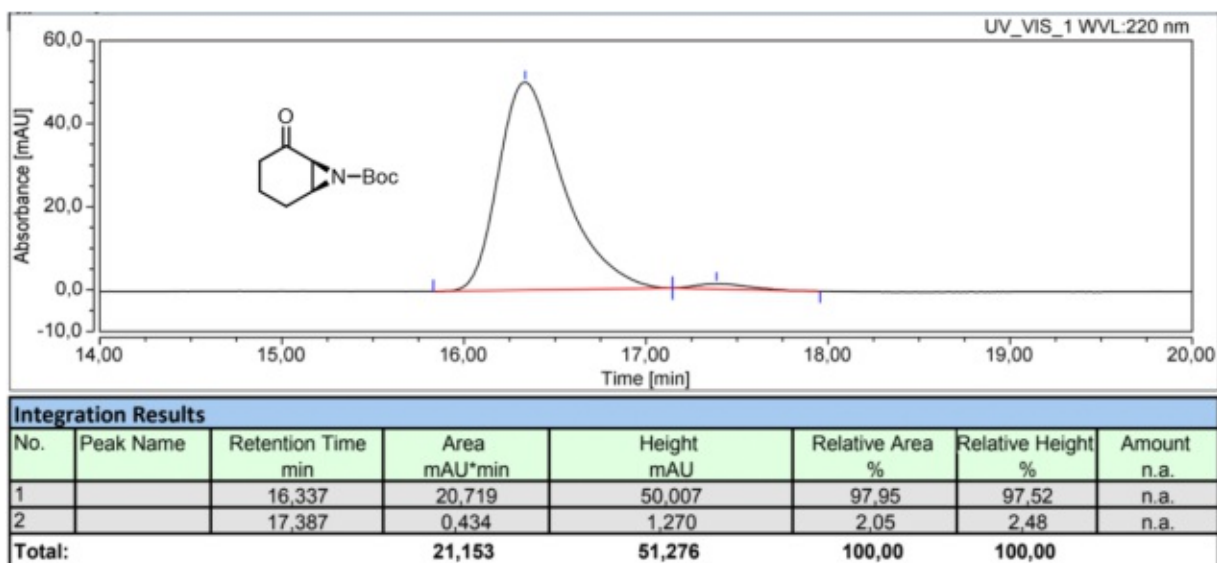
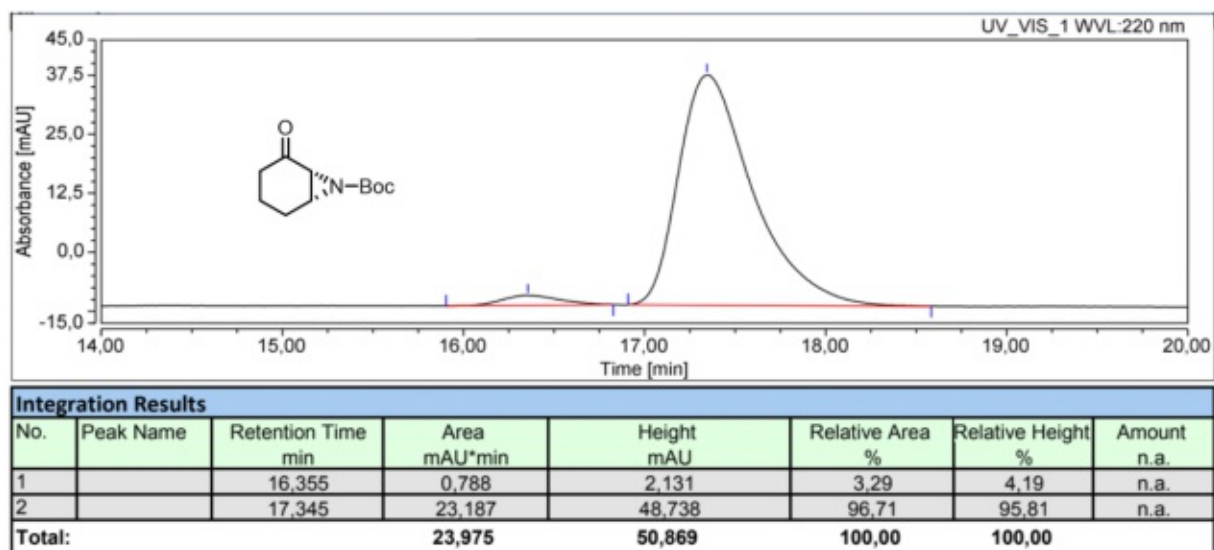
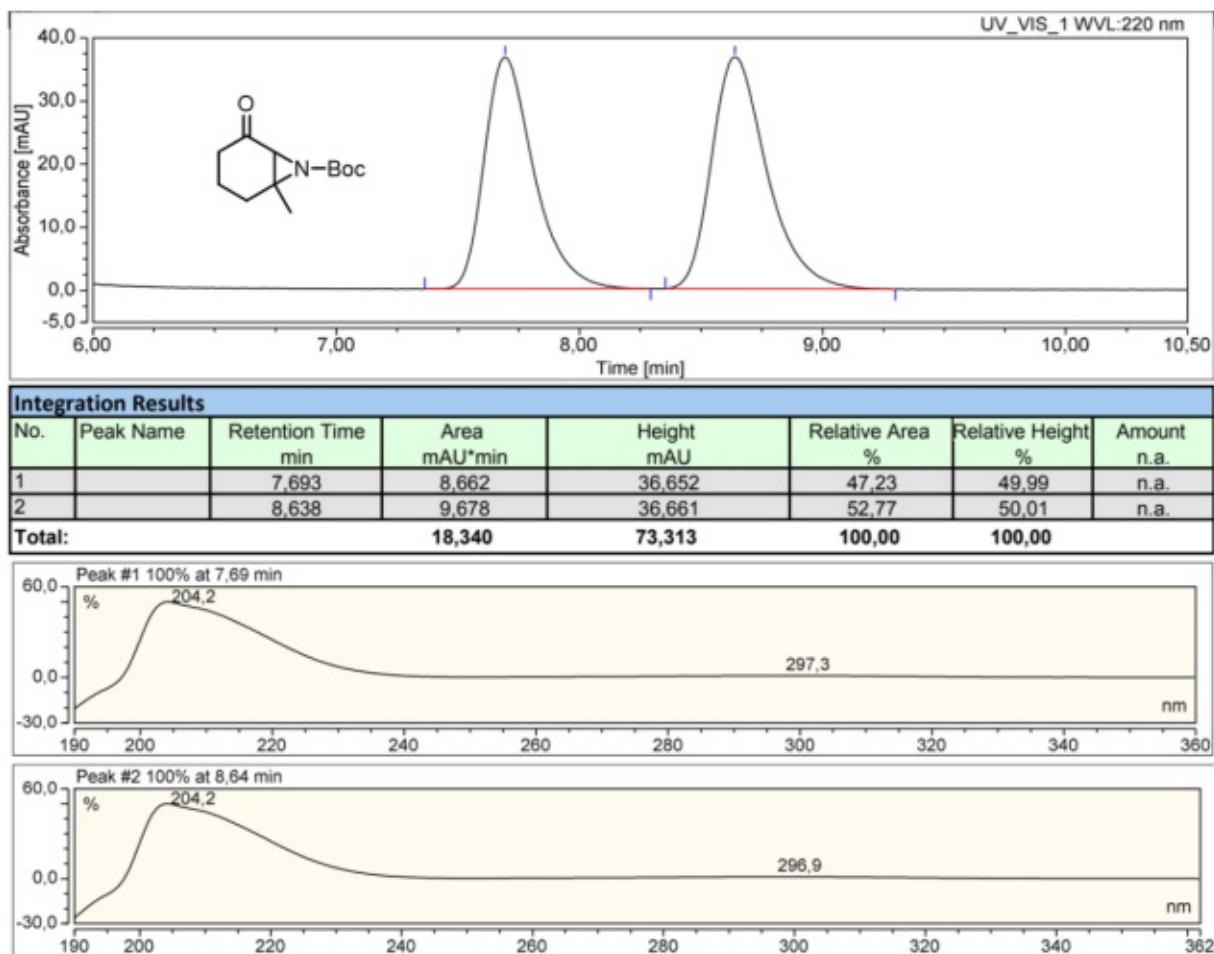


Figure 48: HPLC chromatogram of the racemic *tert*-butyl-2-oxo-7-azabicyclo[4.1.0]heptane-7-carboxylate.

Figure 49: HPLC chromatogram of *tert*-butyl (1*S*,6*S*)-2-oxo-7-azabicyclo[4.1.0]heptane-7-carboxylate.Figure 50: HPLC chromatogram of *tert*-butyl (1*R*,6*R*)-2-oxo-7-azabicyclo[4.1.0]heptane-7-carboxylate.

7.1.2 *tert*-Butyl-1-methyl-5-oxo-7-azabicyclo[4.1.0]heptane-7-carboxylateFigure 51: HPLC chromatogram of the racemic *tert*-butyl-1-methyl-5-oxo-7-azabicyclo[4.1.0]heptane-7-carboxylate.

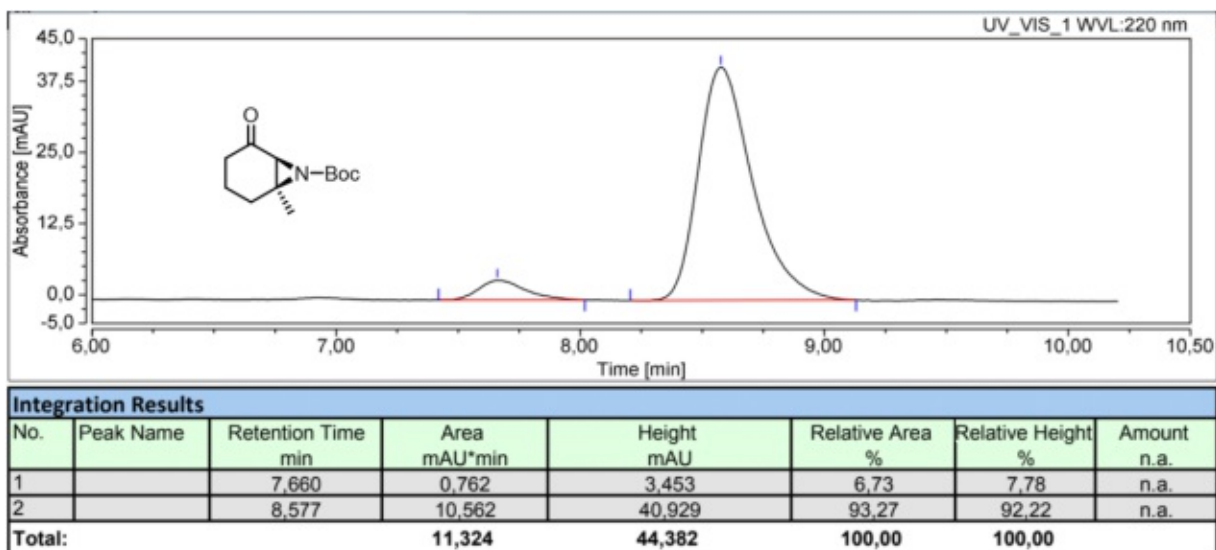


Figure 52: HPLC chromatogram of *tert*-butyl (1*S*,6*S*)-1-methyl-5-oxo-7-azabicyclo[4.1.0]heptane-7-carboxylate.

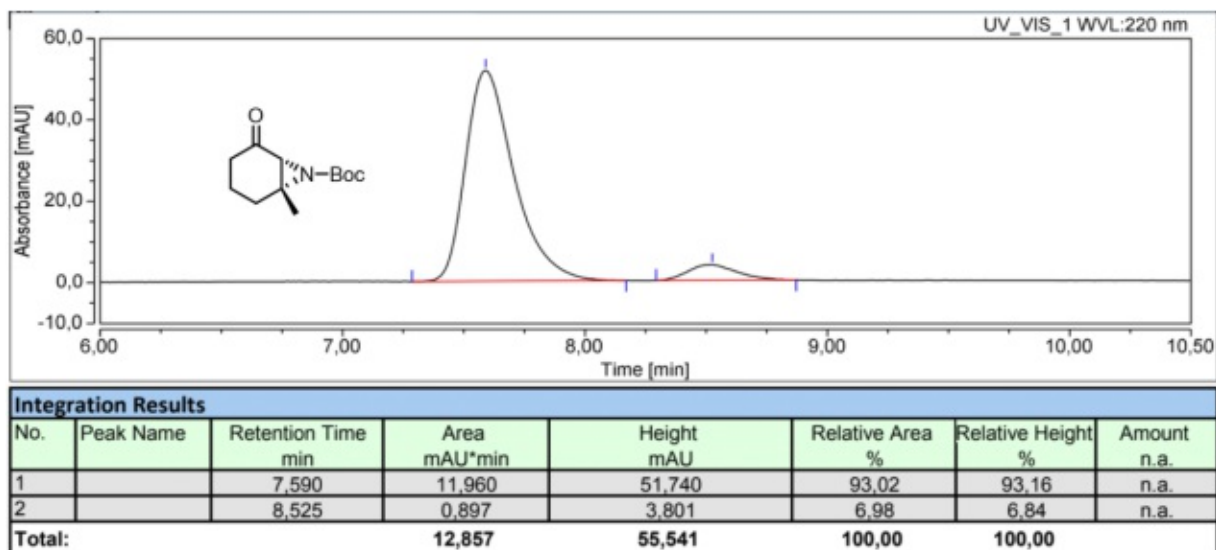
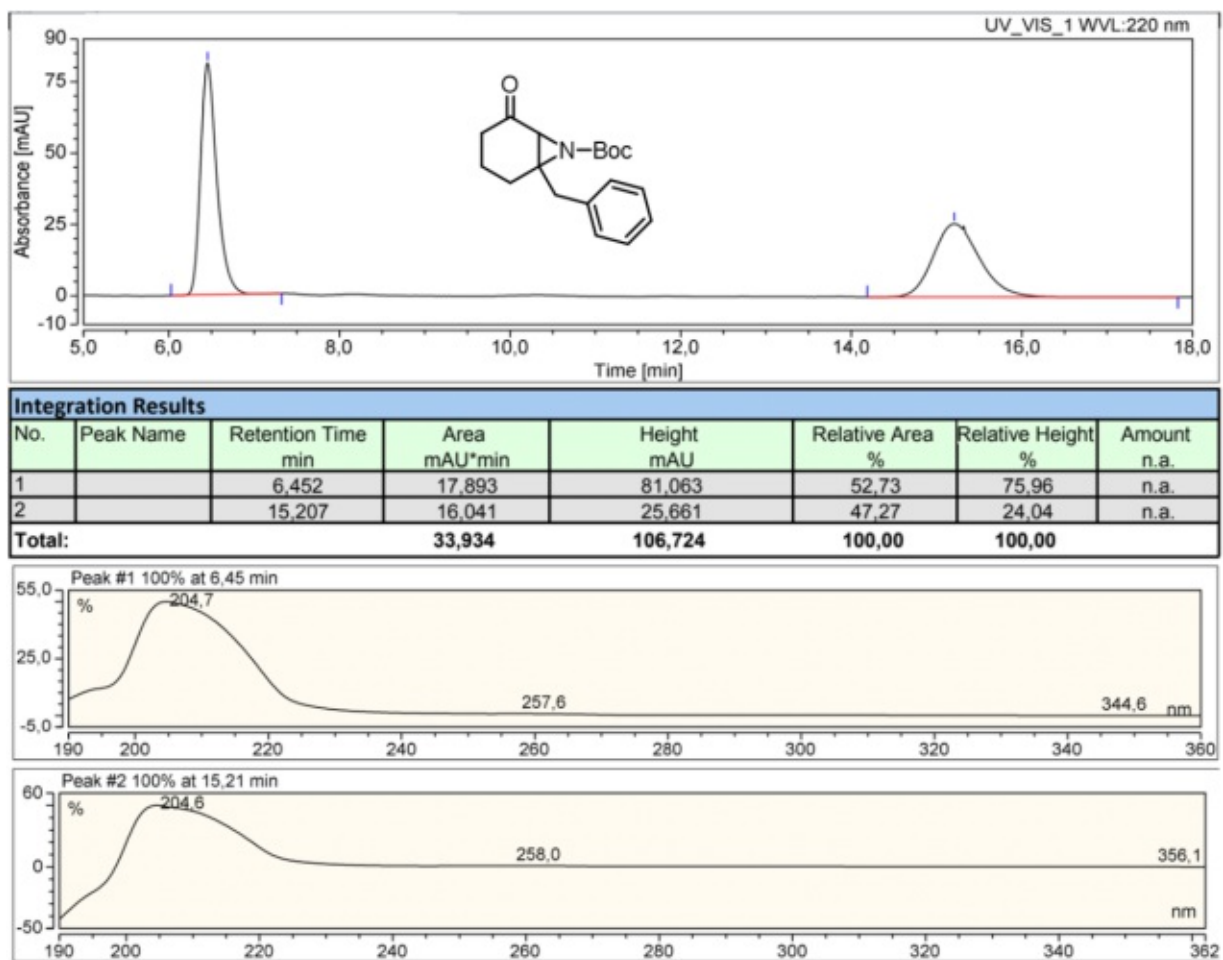


Figure 53: HPLC chromatogram of *tert*-butyl (1*R*,6*R*)-1-methyl-5-oxo-7-azabicyclo[4.1.0]heptane-7-carboxylate.

7.1.3 *tert*-Butyl-1-benzyl-5-oxo-7-azabicyclo[4.1.0]heptane-7-carboxylateFigure 54: HPLC chromatogram of the racemic *tert*-butyl-1-benzyl-5-oxo-7-azabicyclo[4.1.0]heptane-7-carboxylate.

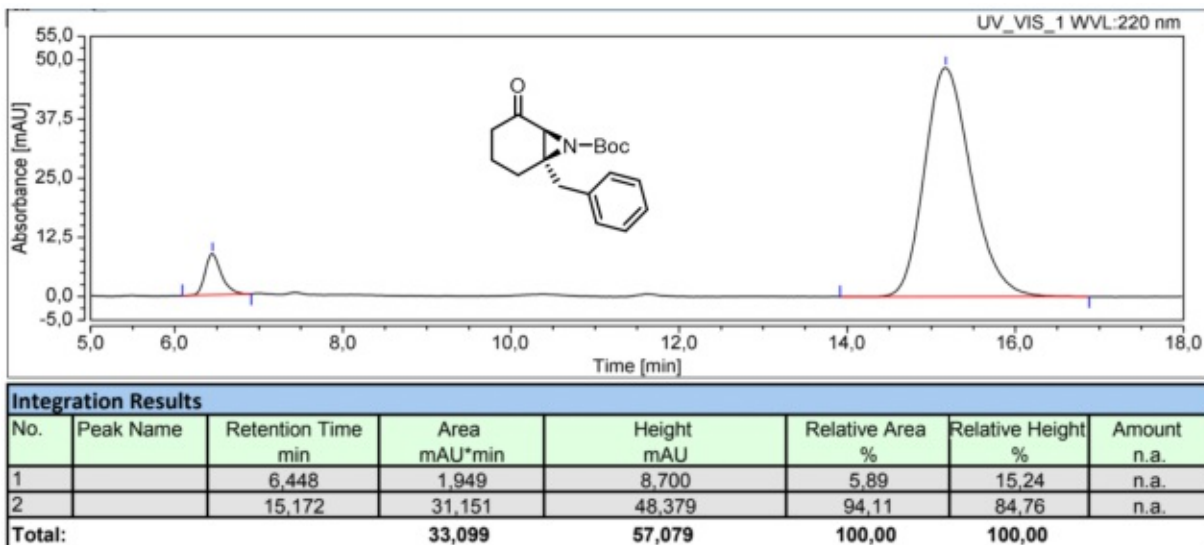


Figure 55: HPLC chromatogram of *tert*-butyl (1*R*,6*S*)-1-benzyl-5-oxo-7-azabicyclo[4.1.0]heptane-7-carboxylate.

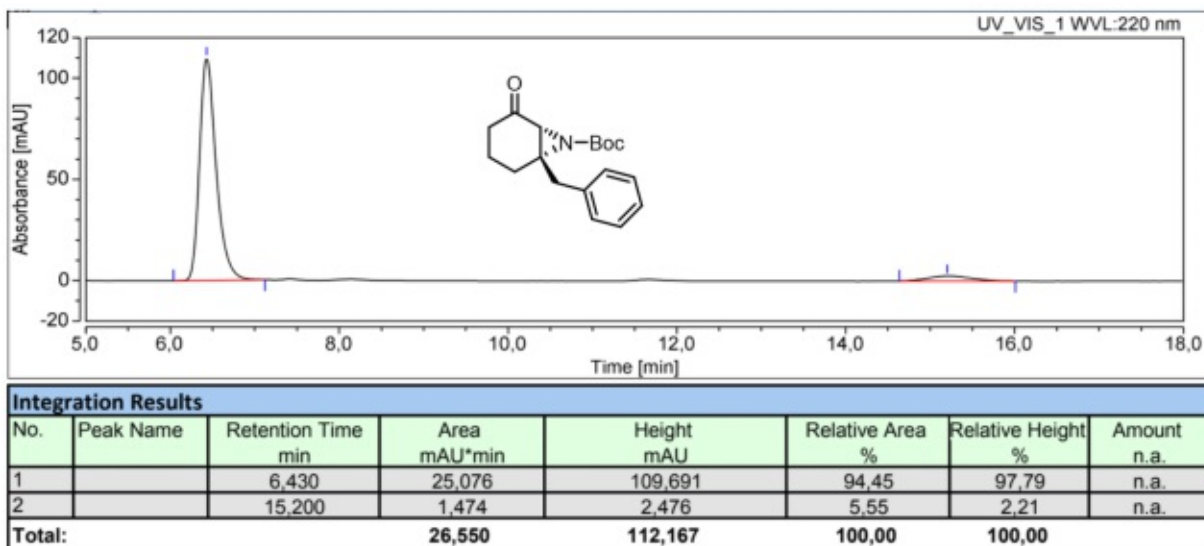
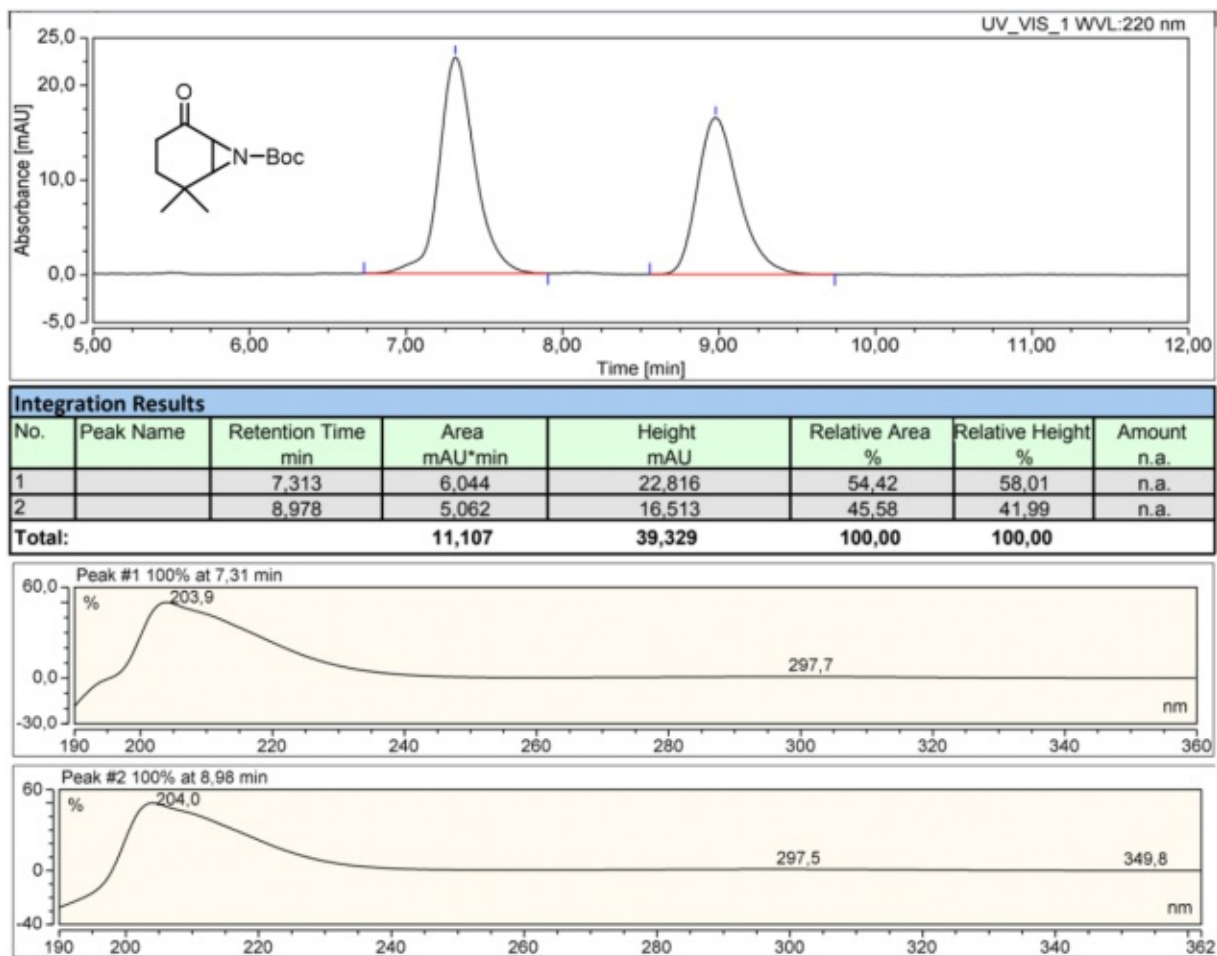


Figure 56: HPLC chromatogram of *tert*-butyl (1*S*,6*R*)-1-benzyl-5-oxo-7-azabicyclo[4.1.0]heptane-7-carboxylate.

7.1.4 *tert*-Butyl-2,2-dimethyl-5-oxo-7-azabicyclo[4.1.0]heptane-7-carboxylateFigure 57: HPLC chromatogram of the racemic *tert*-butyl-2,2-dimethyl-5-oxo-7-azabicyclo[4.1.0]heptane-7-carboxylate.

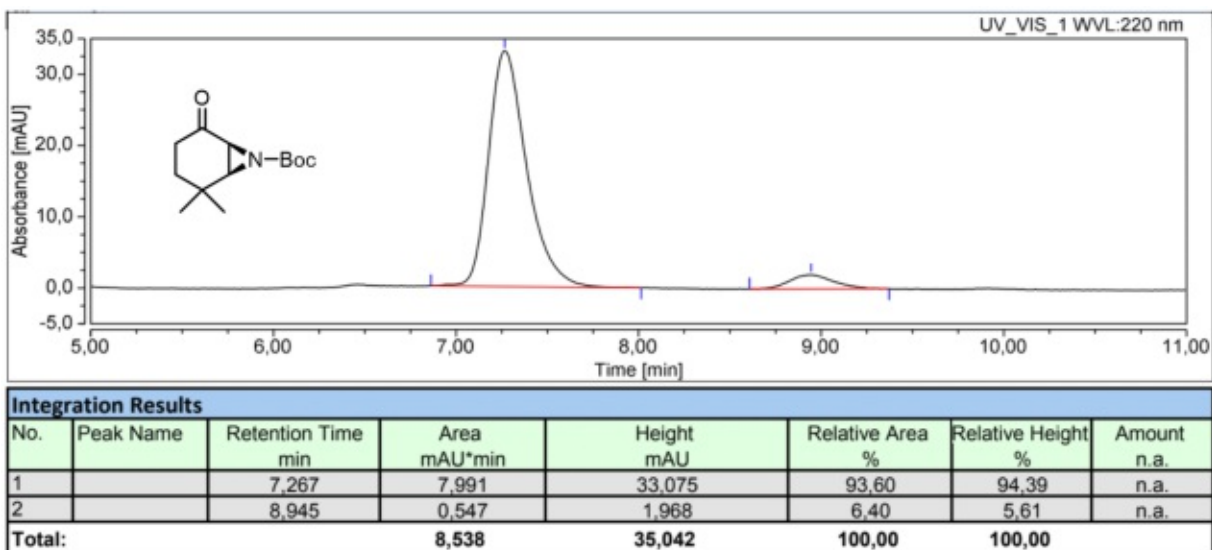


Figure 58: HPLC chromatogram of *tert*-butyl (1*S*,6*S*)-2,2-dimethyl-5-oxo-7-azabicyclo[4.1.0]heptane-7-carboxylate.

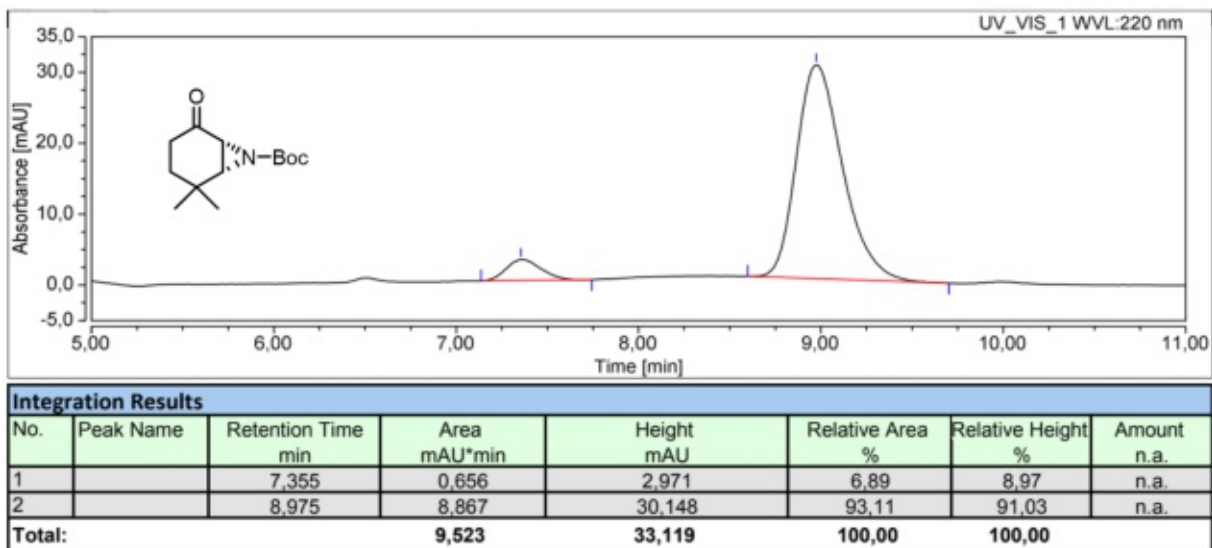


Figure 59: HPLC chromatogram of *tert*-butyl (1*R*,6*R*)-2,2-dimethyl-5-oxo-7-azabicyclo[4.1.0]heptane-7-carboxylate.

7.2 List of abbreviations

AcCl	acetyl chloride
AcOH	acetic acid
Al ₂ O ₃	aluminum oxide
BINOL	1,1'-bi-2-naphthol
Boc ₂ O	di- <i>tert</i> -butylcarbonate
CAN	ceric(IV) ammonium nitrate
Cbz	carboxybenzyl
CDCl ₃	deuterated chloroform
CHCl ₃	chloroform
CH ₃ CN	acetonitrile
conv.	conversion
DCC	dicyclohexylcarbodiimide
DCE	1,2-dichloroethane
DCM	dichloromethane
DCU	dicyclohexylurea
ee	enantiomeric excess
equiv.	molar equivalents
Et ₃ N	triethylamine
Et ₂ O	diethyl ether
EtOAc	ethyl acetate
EtOH	ethanol
HCl	hydrochloric acid
H ₂ O	water
HOBt	1-hydroxybenzotriazole
HOMO	highest occupied molecular orbital
HPLC	high pressure liquid chromatography
LG	leaving group
LiAlH ₄	lithium aluminium hydride
LUMO	lowest unoccupied molecular orbital
MeOH	methanol
MTBE	methyl <i>tert</i> -butyl ether
Na ₂ CO ₃	sodium carbonate
NaHCO ₃	sodium hydrogen carbonate
NaNO ₂	sodium nitrite

NaOH	sodium hydroxide
Na ₂ SO ₄	sodium sulfate
<i>N</i> -PMP	<i>N</i> - <i>p</i> -methoxyphenyl
Ns	nosyl
PE	petroleum ether
PhI	iodobenzene
PhI=NTs	[<i>N</i> -(<i>p</i> -toluenesulfonyl)imino]phenyliodinane
POCl ₃	phosphoryl chloride
r.t.	room temperature
SET	single-electron transfer
SOMO	singly occupied molecular orbital
TFA	trifluoro acetic acid
THF	tetrahydrofuran
TsCl	tosyl chloride

7.3 List of figures

Figure 1	Ring strains in three-membered rings. ³	1
Figure 2	“Banana” shaped bonds. ³	2
Figure 3	Ring opening reactions of aziridines. ¹	2
Figure 4	Examples of biologically-active aziridine-containing compounds and compounds obtained from aziridines. ¹	3
Figure 5	Asymmetric catalytic aziridination performed by Evans. ⁶	4
Figure 6	Asymmetric aziridines produced from 1,2-azidoalcohols. ⁵	5
Figure 7	Aziridine synthesis via carbene addition to imines. ²	5
Figure 8	Aziridine synthesis via ylide addition to imines. ⁴	6
Figure 9	General scheme for the organocatalytic asymmetric aziridination of α,β -unsaturated carbonyl compounds. ¹	6
Figure 10	The three classes of asymmetric catalysis.	7
Figure 11	Quinine and quinidine, used as organocatalysts. ¹⁴	7
Figure 12	Organocatalytic addition of methanol to phenylmethylketene. ¹⁴	8
Figure 13	Hajos-Parrish-Eder-Sauer-Wiechert reaction. ¹⁴	8
Figure 14	Overview of organocatalytic activation modes.	10
Figure 15	Examples of catalysts used in enamine catalysis. ¹⁸	11
Figure 16	Catalytic cycle of the enamine activation. ¹⁷	11
Figure 17	H-bond vs steric directing group. ¹⁹	12
Figure 18	General scheme of iminium catalysis. ²¹	13
Figure 19	Collection of catalysts used for iminium catalysis. ²⁰	13
Figure 20	Catalytic cycle of the iminium activation. ²¹	14
Figure 21	Influence of steric interactions in the pyrrolidine catalyzed β -functionalization of α,β -unsaturated aldehydes. ¹⁹	14
Figure 22	General scheme of the iminium-enamine activation. ²²	15
Figure 23	Example for an α -halogenation reaction. ²³	15
Figure 24	Imidazolidinone catalysts used by MacMillan. ²³	15
Figure 25	Overview of the activation modes in amine catalysis. ²⁵	16
Figure 26	Catalytic cycle of SOMO catalysis. ²⁵	17
Figure 27	General principle of ACDC. ²⁷	18
Figure 28	Different types of ion pairs. ²⁹	18
Figure 29	ACDC in iminium catalysis. ¹¹	19
Figure 30	Examples of BINOL-derived phosphoric acid counteranions. ²⁹	19
Figure 31	ACDC-mediated transfer hydrogenation of α,β -unsaturated aldehydes. ³⁰	20

Figure 32	Counterion enhanced organocatalytic asymmetric transfer hydrogenation using Hantzsch ethyl ester as reductant. ³¹	21
Figure 33	MacMillan's and List's catalyst systems for the asymmetric transfer hydrogenation. ³¹	21
Figure 34	Catalyst system for the counterion enhanced organocatalysis. ³¹	22
Figure 35	Asymmetric α -allylation of α -branched aldehydes. ³³	22
Figure 36	General scheme for the asymmetric aziridination of cyclic enones. ³⁴	23
Figure 37	State-of-the-art catalyst systems for the asymmetric aziridination. ³⁴	23
Figure 38	General catalyst scheme for the asymmetric counterion enhanced organocatalytic aziridination.	24
Figure 39	General reaction scheme for the catalyst optimization.	25
Figure 40	Proposed hydrogen-bonding interactions between the catalyst and the reactant.	27
Figure 41	Acid equivalents screening.	29
Figure 42	Optimized catalyst system.	33
Figure 43	Catalyst components used for the asymmetric aziridination of cyclic enones.	38
Figure 44	Reaction scheme of the diamine synthesis.	39
Figure 45	Reaction scheme of the phosphoric acid synthesis.	40
Figure 46	Proposed mechanism for the asymmetric aziridination.	43
Figure 47	Asymmetric aziridination of cyclic enones via counterion enhanced organocatalysis with the optimized catalyst system.	45
Figure 48	HPLC chromatogram of the racemic <i>tert</i> -butyl-2-oxo-7-azabicyclo[4.1.0]-heptane-7-carboxylate.	66
Figure 49	HPLC chromatogram of <i>tert</i> -butyl (1 <i>S</i> ,6 <i>S</i>)-2-oxo-7-azabicyclo[4.1.0]-heptane-7-carboxylate.	67
Figure 50	HPLC chromatogram of <i>tert</i> -butyl (1 <i>R</i> ,6 <i>R</i>)-2-oxo-7-azabicyclo[4.1.0]-heptane-7-carboxylate.	67
Figure 51	HPLC chromatogram of the racemic <i>tert</i> -butyl-1-methyl-5-oxo-7-azabicyclo[4.1.0]heptane-7-carboxylate.	68
Figure 52	HPLC chromatogram of <i>tert</i> -butyl (1 <i>S</i> ,6 <i>S</i>)-1-methyl-5-oxo-7-azabicyclo[4.1.0]heptane-7-carboxylate.	69
Figure 53	HPLC chromatogram of <i>tert</i> -butyl (1 <i>R</i> ,6 <i>R</i>)-1-methyl-5-oxo-7-azabicyclo[4.1.0]heptane-7-carboxylate.	69
Figure 54	HPLC chromatogram of the racemic <i>tert</i> -butyl-1-benzyl-5-oxo-7-azabicyclo[4.1.0]heptane-7-carboxylate.	70

Figure 55	HPLC chromatogram of <i>tert</i> -butyl (1 <i>R</i> ,6 <i>S</i>)-1-benzyl-5-oxo-7-azabicyclo[4.1.0]heptane-7-carboxylate.	71
Figure 56	HPLC chromatogram of <i>tert</i> -butyl (1 <i>S</i> ,6 <i>R</i>)-1-benzyl-5-oxo-7-azabicyclo[4.1.0]heptane-7-carboxylate.	71
Figure 57	HPLC chromatogram of the racemic <i>tert</i> -butyl-2,2-dimethyl-5-oxo-7-azabicyclo[4.1.0]heptane-7-carboxylate.	72
Figure 58	HPLC chromatogram of <i>tert</i> -butyl (1 <i>S</i> ,6 <i>S</i>)-2,2-dimethyl-5-oxo-7-azabicyclo[4.1.0]heptane-7-carboxylate.	73
Figure 59	HPLC chromatogram of <i>tert</i> -butyl (1 <i>R</i> ,6 <i>R</i>)-2,2-dimethyl-5-oxo-7-azabicyclo[4.1.0]heptane-7-carboxylate.	73

7.4 List of tables

Table 1	Comparison between organocatalysis and transition-metal catalysis. ¹⁵	9
Table 2	Optimization of the amine-functionality.	26
Table 3	Optimization of the acid-derived anion.	28
Table 4	Catalyst screening 1.	31
Table 5	Catalyst screening 2.	32
Table 6	Base and base equivalents screening.	34
Table 7	Solvent screening.	35
Table 8	Optimization of the reactant.	37
Table 9	Substrate scope.	42

8 References

- [1] Roma, E.; Tosi, E.; Miceli, M.; Gasperi, T. Asymmetric Organocatalytic Aziridination: Recent Advances. *Asian J. Org. Chem.* **2018**, *7*, 2357–2367.
- [2] Degennaro, L.; Trinchera, P.; Luisi, R. Recent Advances in the Stereoselective Synthesis of Aziridines. *Chem. Rev.* **2014**, *114*, 7881–7929.
- [3] Talukdar, R. Synthetically important ring opening reactions by alkoxybenzenes and alkoxy-naphthalenes. *RSC Adv.* **2020**, *10*, 31363–31376.
- [4] Pellissier, H. Recent Developments in Asymmetric Aziridination. *Adv. Synth. Catal.* **2014**, *356*, 1899–1935.
- [5] Sweeney, J. B. Aziridines: epoxides' ugly cousins? *Chem. Soc. Rev.* **2002**, *31*, 247–258.
- [6] Evans, D. A.; Faul, M. M.; Bilodeau, M. T. Development of the Copper-Catalyzed Olefin Aziridination Reaction. *J. Am. Chem. Soc.* **1994**, *116*, 2742–2753.
- [7] Hansen, K. B.; Finney, N. S.; Jacobsen, E. N. Carbenoid Transfer to Imines: A New Asymmetric Catalytic Synthesis of Aziridines. *Angew. Chem. Int. Ed.* **1995**, *34*, 676–678.
- [8] Rasmussen, K. G.; Jørgensen, K. A. Catalytic Formation of Aziridines from Imines and Diazoacetate. *J. Chem. Soc., Chem. Commun.* **1995**, 1401–1402.
- [9] Zhang, X. J.; Yan, M.; Huang, D. Catalyzed addition of diazoacetoacetates to imines: synthesis of highly functionalized aziridines. *Org. Biomol. Chem.* **2009**, *7*, 187–192.
- [10] Xue, Z.; Dee, V. M.; Hope-Weeks, L. J.; Whittlesey, B. R.; Mayer, M. F. Asymmetric aziridination of *N*-*tert*-butanesulfinyl imines with phenyldiazomethane via sulfur ylides. *Arkivoc* **2010**, *vii*, 65–80.
- [11] Pan, S. C.; List, B. *New Concepts for Organocatalysis*. In: Reetz M., List B., Jaroch S., Weinmann H. (eds) *Organocatalysis. Ernst Schering Foundation Symposium Proceedings*; Springer, Berlin, Heidelberg, 2007; pp 259–300.
- [12] Pellissier, H. Asymmetric organocatalysis. *Tetrahedron* **2007**, *63*, 9267–9331.
- [13] MacMillan, D. W. The advent and development of organocatalysis. *Nature* **2008**, *455*, 304–308.
- [14] Berkessel, A.; Gröger, H. *Asymmetric Organocatalysis: From Biomimetic Concepts to Powerful Methods in Asymmetric Synthesis*; Wiley-VCH, 2005; pp 1–8.

- [15] Shaikh, I. R. Organocatalysis: Key Trends in Green Synthetic Chemistry, Challenges, Scope towards Heterogenization, and Importance from Research and Industrial Point of View. *J. Catal.* **2014**, *2014*, 1–35.
- [16] Palumbo, C.; Guidotti, M. Organocatalysts for enantioselective synthesis of fine chemicals: definitions, trends and developments. *Sci. Res.* **2015**, 1–14.
- [17] List, B. Enamine Catalysis Is a Powerful Strategy for the Catalytic Generation and Use of Carbanion Equivalents. *Acc. Chem. Res.* **2004**, *37*, 548–557.
- [18] Seayad, J.; List, B. Asymmetric organocatalysis. *Org. Biomol. Chem.* **2005**, *3*, 719–724.
- [19] Bertelsen, S.; Jørgensen, K. A. Organocatalysis-after the gold rush. *Chem. Soc. Rev.* **2009**, *38*, 2178–2189.
- [20] Erkkilä, A.; Majander, I.; Pihko, P. M. Iminium Catalysis. *Chem. Rev.* **2007**, *107*, 5416–5470.
- [21] List, B. The ying and yang of asymmetric aminocatalysis. *Chem. Commun.* **2006**, 819–824.
- [22] Enders, D.; Grondal, C.; Hüttl, M. R. Asymmetric Organocatalytic Domino Reactions. *Angew. Chemie - Int. Ed.* **2007**, *46*, 1570–1581.
- [23] Huang, Y.; Walji, A. M.; Larsen, C. H.; MacMillan, D. W. Enantioselective Organocascade Catalysis. *J. Am. Chem. Soc.* **2005**, *127*, 15051–15053.
- [24] Jang, H. Y.; Hong, J. B.; MacMillan, D. W. Enantioselective Organocatalytic Singly Occupied Molecular Orbital Activation: The Enantioselective α -Enolation of Aldehydes. *J. Am. Chem. Soc.* **2007**, *129*, 7004–7005.
- [25] MacMillan, D. W.; Rendler, S. *Enantioselective Organo-SOMO Catalysis: A Novel Activation Mode for Asymmetric Synthesis*. In: *Asymmetric Synthesis*; Wiley-VCH, 2013; pp 87–94.
- [26] Mahlau, M.; List, B. Asymmetric Counteranion-Directed Catalysis: Concept, Definition, and Applications. *Angew. Chemie - Int. Ed.* **2013**, *52*, 518–533.
- [27] Mahlau, M.; List, B. *Asymmetric Counteranion-Directed Catalysis (ACDC)*. In: *Asymmetric Synthesis*; Wiley-VCH, 2012; pp 79–85.
- [28] Mahlau, M.; List, B. Asymmetric Counteranion-Directed Catalysis (ACDC): A Remarkably General Approach to Enantioselective Synthesis. *Isr. J. Chem.* **2012**, *52*, 630–638.

- [29] Brak, K.; Jacobsen, E. N. Asymmetric Ion-Pairing Catalysis. *Angew. Chemie - Int. Ed.* **2013**, *52*, 534–561.
- [30] Mayer, S.; List, B. Asymmetric Counteranion-Directed Catalysis. *Angew. Chemie - Int. Ed.* **2006**, *45*, 4193–4195.
- [31] Scharinger, F.; Pálvölgyi, Á. M.; Zeindlhofer, V.; Schnürch, M.; Schröder, C.; Bica-Schröder, K. Counterion Enhanced Organocatalysis: A Novel Approach for the Asymmetric Transfer Hydrogenation of Enones. *ChemCatChem* **2020**, *12*, 3776–3782.
- [32] Ouellet, S. G.; Tuttle, J. B.; MacMillan, D. W. Enantioselective Organocatalytic Hydride Reduction. *J. Am. Chem. Soc.* **2005**, *127*, 32–33.
- [33] Pálvölgyi, Á. M.; Smith, J.; Schnürch, M.; Bica-Schröder, K. Counterion-Enhanced Pd/Enamine Catalysis: Direct Asymmetric α -Allylation of Aldehydes with Allylic Alcohols by Chiral Amines and Achiral or Racemic Phosphoric Acids. *J. Org. Chem.* **2021**, *86*, 850–860.
- [34] De Vincentiis, F.; Bencivenni, G.; Pesciaioli, F.; Mazzanti, A.; Bartoli, G.; Galzerano, P.; Melchiorre, P. Asymmetric Catalytic Aziridination of Cyclic Enones. *Chem. Asian J.* **2010**, *5*, 1652–1656.
- [35] Haraguchi, N.; Takenaka, N.; Najwa, A.; Takahara, Y.; Mun, M. K.; Itsuno, S. Synthesis of Main-Chain Ionic Polymers of Chiral Imidazolidinone Organocatalysts and Their Application to Asymmetric Diels-Alder Reactions. *Adv. Synth. Catal.* **2018**, *360*, 112–123.
- [36] Hatano, M.; Miyamoto, T.; Ishihara, K. Highly Active Chiral Phosphoramidate - Zn(II) Complexes as Conjugate Acid - Base Catalysts for Enantioselective Organozinc Addition to Ketones. *Org. Lett.* **2007**, *9*, 4535–4538.
- [37] Khatik, G. L.; Kumar, V.; Nair, V. A. Reversal of Selectivity in Acetate Aldol Reactions of *N*-Acetyl-(*S*)-4-isopropyl-1-[(*R*)-1-phenylethyl]imidazolidin-2-one. *Org. Lett.* **2012**, *14*, 2442–2445.
- [38] Davis, T. J.; Balsells, J.; Carroll, P. J.; Walsh, P. J. Optimization of Asymmetric Catalysts Using Achiral Ligands: Metal Geometry-Induced Ligand Asymmetry. *Org. Lett.* **2001**, *3*, 2161–2164.
- [39] Gutierrez, E. G.; Moorhead, E. J.; Smith, E. H.; Lin, V.; Ackerman, L. K.; Knezevic, C. E.; Sun, V.; Grant, S.; Wenzel, A. G. Electron-Withdrawing, Biphenyl-2,2'-diol-Based Compounds for Asymmetric Catalysis. *Eur. J. Org. Chem.* **2010**, *1*, 3027–3031.

- [40] Behr, J. B.; Chevrier, C.; Defoin, A.; Tarnus, C.; Streith, J. Asymmetric synthesis of potent glycosidase and very potent α -mannosidase inhibitors: 4-amino-4-deoxy-L-erythrose and 4-amino-4,5-dideoxy-L-ribose. *Tetrahedron* **2003**, *59*, 543–553.
- [41] Ma, X.; Hazelden, I. R.; Langer, T.; Munday, R. H.; Bower, J. F. Enantioselective Aza-Heck Cyclizations of *N*-(Tosyloxy)carbamates: Synthesis of Pyrrolidines and Piperidines. *J. Am. Chem. Soc.* **2019**, *141*, 3356–3360.
- [42] Wang, A.; Venditto, N. J.; Darcy, J. W.; Emmert, M. H. Nondirected, Cu-Catalyzed sp^3 C-H Aminations with Hydroxylamine-Based Amination Reagents: Catalytic and Mechanistic Studies. *Organometallics* **2017**, *36*, 1259–1268.
- [43] Felber, M.; Bauwens, M.; Mateos, J. M.; Imstepf, S.; Mottaghy, F. M.; Alberto, R. ^{99m}Tc Radiolabeling and Biological Evaluation of Nanoparticles Functionalized with a Versatile Coating Ligand. *Chem. Eur. J.* **2015**, *21*, 6090–6099.